

AD-A095 357

PRATT AND WHITNEY AIRCRAFT GROUP WEST PALM BEACH FL 8--ETC F/6 13/9
HIGH SPEED CYLINDRICAL ROLLER BEARING DEVELOPMENT.(U)

AUG 80 P F BROWN, L J DOBEK, E J TOBIASZ F33615-77-C-3114
PWA-FR-12598 AFWAL-TR-80-2072 NL

UNCLASSIFIED

1 of 1
AD-A095 357

END
DATE
FILMED
4-81
DTIC

AD A095357

AFWAL-TR-80-2072

LEVEL II

2

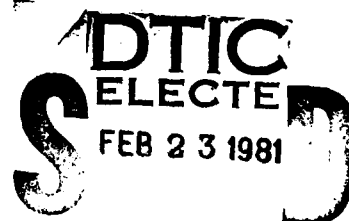
HIGH SPEED CYLINDRICAL ROLLER BEARING DEVELOPMENT

United Technologies Corporation
Pratt & Whitney Aircraft Group
Government Products Division
West Palm Beach, Florida 33402



August 1980

TECHNICAL REPORT AFWAL-TR-80-2072
Final Report for Period 15 September 1977 - 29 February 1980



Approved for public release; distribution unlimited

DBG FILE COPY

AERO PROPULSION LABORATORY
AIR FORCE WRIGHT AERONAUTICAL LABORATORIES
AIR FORCE SYSTEMS COMMAND
WRIGHT-PATTERSON AIR FORCE BASE, OHIO 45433


81 2 23 101

NOTICE

When Government drawings, specifications, or other data are used for any purpose other than in connection with a definitely related Government procurement operation, the United States Government thereby incurs no responsibility nor any obligation whatsoever; and the fact that the government may have formulated, furnished, or in any way supplied the said drawings, specifications, or other data, is not to be regarded by implication or otherwise as in any manner licensing the holder or any other person or corporation, or conveying any rights or permission to manufacture use, or sell any patented invention that may in any way be related thereto.


This report has been reviewed by the Office of Public Affairs (ASD/PA) and is releasable to the National Technical Information Service (NTIS). At NTIS, it will be available to the general public, including foreign nations.

This technical report has been reviewed and is approved for publication.


RONALD D. DAYTON
Project Engineer


HOWARD F. JONES, Chief
Lubrication Branch

FOR THE COMMANDER


ROBERT D. SHERRILL, Chief
Fuels & Lubrication Division

"If your address has changed, if you wish to be removed from our mailing list, or if the addressee is no longer employed by your organization please notify AFMIL/POST W-PAFB, OH 45433 to help us maintain a current mailing list".

Copies of this report should not be returned unless return is required by security considerations, contractual obligations, or notice on a specific document.

SECURITY CLASSIFICATION OF THIS PAGE (When Data Entered)

(14) PWA-FR-12598

19 REPORT DOCUMENTATION PAGE		READ INSTRUCTIONS BEFORE COMPLETING FORM
1. REPORT NUMBER (18) AFWALTR-80-2872	2. GOVT ACCESSION NO. AD-A095357	3. RECIPIENT'S CATALOG NUMBER
4. TITLE (and Subtitle) (6) High Speed Cylindrical Roller Bearing Development	5. TYPE OF REPORT & PERIOD COVERED (9) Final report. 15 September 1977 to 29 February 1980	6. PERFORMING ORG. REPORT NUMBER FR-12598
7. AUTHOR(s) (10) Paul F. Brown Louis J. Dobek Edward J. Tobiasz	8. CONTRACT OR GRANT NUMBER(s) (15) F33615-77-C-3114	
9. PERFORMING ORGANIZATION NAME AND ADDRESS United Technologies Corporation Pratt & Whitney Aircraft Group Government Products Division West Palm Beach, Florida 33402	10. PROGRAM ELEMENT, PROJECT, TASK AREA & WORK UNIT NUMBERS (16) 3948 06 01	
11. CONTROLLING OFFICE NAME AND ADDRESS Aero Propulsion Laboratory AF Wright Aeronautical Laboratories Wright-Patterson AFB, Ohio 45433	12. REPORT DATE March 1980 (11) Aug 80	
14. MONITORING AGENCY NAME & ADDRESS (if different from Controlling Office) (12) 72 (17) 06	13. NUMBER OF PAGES 72	15. SECURITY CLASS. (of this report) Unclassified
16. DISTRIBUTION STATEMENT (of this Report) Approved for public release: Distribution unlimited.		15a. DECLASSIFICATION/DOWNGRADING SCHEDULE
17. DISTRIBUTION STATEMENT (of the abstract entered in Block 20, if different from Report)		
18. SUPPLEMENTARY NOTES		
19. KEY WORDS (Continue on reverse side if necessary and identify by block number) <ul style="list-style-type: none"> • Cylindrical roller bearing • Gas turbine mainshaft roller bearing • High speed roller bearing • Dynamics • Roller end wear 		
20. ABSTRACT (Continue on reverse side if necessary and identify by block number) <p>High speed experimental tests provided data on six parametric cylindrical roller bearings. Four bearing variables were evaluated and the results were correlated with the analytical model developed under Naval Air Propulsion Center Contract N00140-78-C-0383 with support from the Air Force Aero Propulsion Laboratory MIPR FY14557600623. Roller end clearance was found to have a significant effect on roller end and guide flange wear, whereas the variables roller end circular runout and inner ring guide flange height were both observed to have a moderate effect on wear.</p>		

DD Form
1 JAN 78

1473

EDITION OF 1 NOV 65 IS OBSOLETE

SECURITY CLASSIFICATION OF THIS PAGE (When Data Entered)

392887

gm

FOREWORD

This report describes the work performed by the Pratt & Whitney Aircraft Group, Government Products Division of United Technologies Corporation, West Palm Beach, Florida, 33402, under U. S. Air Force Contract F33615-77-C-3114. The contract was initiated under Project 3048, "Fuels, Lubrication, and Fire Protection," Task 304806, "Aerospace Lubrication," Work Unit 30480601, "High Speed Cylindrical Roller Bearing Development." This report is submitted in accordance with Section F, Paragraph 5.1 of the contract and Sequence No. 5 of DD Form 1423, and covers the work performed from 15 September 1977 to 29 February 1980.

The Government technical manager for this program was Ronald D. Dayton of the Air Force Aero Propulsion Laboratory, WPAFB (telephone 513-255-4939). The project was conducted at Pratt & Whitney Aircraft under the direction of John Miner, Component Technology Manager; Paul Brown, Principal Investigator; and Louis Dobek, Program Manager. The experimental bearing testing was conducted by Edward Tobiasz who was assisted by Richard Fair and Robert Cohen. John Robinson provided analytical support for this program while Frederick Dauser assisted with the statistical analysis of the experimental wear data.

Acknowledgement is accorded the Split Ballbearing Division of MPB Corporation which provided the experimental hardware for this program.

Accession For	
NTIS GRA&I	<input checked="checked" type="checkbox"/>
DTIC TAB	<input type="checkbox"/>
Unannounced	<input type="checkbox"/>
Justification	
By	
Distribution/	
Availability Codes	
Dist	Avail and/or Special
A	

TABLE OF CONTENTS

<i>Section</i>	<i>Page</i>
SUMMARY	ix
I INTRODUCTION	1
Background	1
Program Approach	4
Design Requirements	4
Program Scope	7
II PARAMETRIC AND VERIFICATION TESTING — PHASE I	9
Parameter Selection	9
Design of Parametric Bearings	11
Procurement of Bearing Hardware	14
Pretest Preparation and Inspection of Test Bearings	16
Roller Bearing Test Rig and Instrumentation	17
Experimental Program Plan	21
Bearing Parametric Tests	22
Experimental Evaluation of Parametric Bearing No. 31	22
Experimental Evaluation of Parametric Bearing No. 27	26
Experimental Evaluation of Parametric Bearing No. 28	29
Experimental Evaluation of Parametric Bearing No. 29	29
Experimental Evaluation of Parametric Bearing No. 30	29
Experimental Evaluation of Parametric Bearing No. 32	38
III BEARING TEST ANALYSIS AND CORRELATION — PHASE II	41
Statistical Analysis of the Experimental Wear Results	41
Correlation of Analytical Model	53
Bearing Heat Generation Correlation	53
Bearing Ring Temperature Correlation	53
IV CONCLUSIONS AND RECOMMENDATIONS	63
Conclusions	63
Recommendations	63
V LIST OF SYMBOLS	65
REFERENCES	66

LIST OF ILLUSTRATIONS

<i>Figure</i>		<i>Page</i>
1	Eccentric Roller End Wear Due to Interaction With the Face of the Inner Ring Guide Flange	2
2	Typical Bearing Failure Attributable to Eccentric Roller End Wear	3
3	Basic Bearing for Parametric and Verification Testing	12
4	Parametric Roller Bearing Designs to Obtain Wear Data on Four Bearing Variables	13
5	High Speed Roller Bearing Test Rig	18
6	Lubrication System for Test Rig	19
7	Cage Slip of Bearing No. 31 Decreases as Applied Load Is Increased With No Skid Observed at Speeds Above 2.75 MDN	23
8	Outer-to-Inner Ring Temperature Differential for Bearing No. 31 Increases With Reduced Oil Supply	23
9	Increasing Oil Flow Results in Increased Heat Generation of Bearing No. 31	24
10	Bearing No. 31 Demonstrates that Increasing Oil Flow Results in Reduced Outer Ring-to-Oil Inlet Temperature Differential	24
11	Concentric Roller End Wear Can Be Observed in Parametric Bearing No. 31. No Skid Damage Was Apparent	25
12	Components of Bearing No. 27 Appear in Good Condition After 10 Hours of Test. Light Concentric Roller End Wear Noted, Except on Several Rollers Where Slight Eccentric Wear Was Observed	27
13	Decreased Roller Skid Is Observed as Radial Load Is Increased on Bearing No. 27. No Skid Was Noted at Speeds Above 2.9 MDN	28
14	Increasing Oil Flow Results in Increased Heat Generation for Bearing No. 27	28
15	Increasing Oil Flow Results in Reduced Outer Ring-to-Oil Inlet Temperature Differential for Bearing No. 27	30
16	Increasing Applied Load Reduces Roller Skid on Bearing No. 28 With No Skidding Above 2.9 MDN	30
17	Increasing Oil Flow Results in Increased Heat Generation for Bearing No. 28	31
18	Increasing Oil Flow Results in Decreased Outer Ring-to-Oil Inlet Temperature Differential for Bearing No. 28	31
19	Components of Bearing No. 28 Appear in Good Condition After 10 Hours of Test. Very Light Eccentric Wear Is Present on Roller Ends	32
20	Increasing Oil Flow Results in Increased Heat Generation for Parametric Bearing Design No. 29	33
21	Increasing Oil Flow Results in Reduced Outer Ring-to-Oil Inlet Temperature Differential for Bearing No. 29	33
22	Components of Parametric Bearing Design No. 29 Appear in Good Condition After 10-Hour Test. Light Concentric and Very Light Eccentric Wear are Present on Roller Ends	34
23	Increasing Applied Load Reduces Roller Skid on Bearing No. 30 With No Skidding Above 2.9 MDN	35
24	Increasing Oil Flow Results in Increased Heat Generation for Bearing No. 30	35
25	Increasing Oil Flow Results in Reduced Outer Ring to Oil Inlet Temperature Differential for Bearing No. 30	36

LIST OF ILLUSTRATIONS (Continued)

Figure		Page
26	Components of Parametric Bearing Design No. 30 Show Low Wear and No Distress After 10-Hour Test. Light Concentric Wear Is Present on Both Ends of Rollers	37
27	Increasing Applied Radial Load Reduces Roller Skid on Bearing No. 32 With No Skidding Above 2.9 MDN.....	38
28	Increasing Oil Flow Results in Increased Heat Generation for Bearing No. 32	39
29	Increasing Oil Flow Results in Reduced Outer Ring-to-Oil Inlet Temperature Differential for Bearing No. 32	39
30	Components of Parametric Bearing Design No. 32 Appear in Good Condition After 10-Hour Test. Light Concentric and Eccentric Wear Observed on Roller Ends.....	40
31	Excellent Correlation Is Shown Between Measured and Predicted Roller Weight Loss	45
32	Excellent Correlation Is Shown Between Measured and Predicted Roller Skew Angle Change	45
33	Curvilinear Effect of Roller End Clearance on Roller Weight Loss	47
34	Inner Ring Guide Flange Height Shows Slight Negative Effect on Roller Weight Loss	47
35	Roller End Circular Runout Shows Slight Negative Effect on Roller Weight Loss.....	48
36	Good Correlation Is Shown Between Roller Weight Loss and Skew Angle Change.....	48
37	Curvilinear Effect of Roller End Clearance on Roller Skew Angle Change.....	49
38	Inner Ring Guide Flange Height Shows Slight Negative Effect on Roller Skew Angle Change	49
39	Initial Roller Skew Angle Shows Positive Effect on Roller Weight Change	50
40	Initial Roller Skew Angle Shows Positive Effect on Roller Skew Angle Change	50
41	Roller End Clearance Shows a Significant Positive Effect on Initial Roller Static Skew Angle	51
42	Inner Ring Guide Flange Height Shows Only a Moderate Negative Effect on Roller Initial Skew Angle	51
43	Bearing Heat Generation Model Identifies Nine Heat Sources Including Drag and Churning Effects Due to Translation and Rotation Through an Air/Oil Environment.....	54
44	The TRIBO-I Thermal Model Provides Good Correlation With Experimental Heat Generation Results (1 of 3).....	55
44	The TRIBO-I Thermal Model Provides Good Correlation With Experimental Heat Generation Results (2 of 3).....	56
44	The TRIBO-I Thermal Model Provides Good Correlation With Experimental Heat Generation Results (3 of 3).....	57
45	The TRIBO-I Thermal Model Allows Prediction of Both Inner and Outer Ring Temperatures to Within 10% of Experimental Results (1 of 4)	58
45	The TRIBO-I Thermal Model Allows Prediction of Both Inner and Outer Ring Temperatures to Within 10% of Experimental Results (2 of 4)	59
45	The TRIBO-I Thermal Model Allows Prediction of Both Inner and Outer Ring Temperatures to Within 10% of Experimental Results (3 of 4)	60
45	The TRIBO-I Thermal Model Allows Prediction of Both Inner and Outer Ring Temperatures to Within 10% of Experimental Results (4 of 4)	61

LIST OF TABLES

<i>Table</i>		<i>Page</i>
1	Relative Ranking of Roller Bearing Variables	6
2	Roller Wear Results from Group-N, Group-AF, and Group-P&WA Tests	10
3	Test Matrix Used in the Design Group-AF4 Parametric Roller Bearings	11
4	Summary of Vendor Manufacturing Inspection Data for Group-AF4 Roller Bearings	15
5	Parametric Roller Bearings — Pretest Wear Related Measurements	16
6	Parametric Roller Bearing Pretest Rig Related Inspection Measurements	16
7	Test Instrumentation	20
8	The Test Program Provides for the Thermal Performance and Short Term Wear Assessment of the Parametric Roller Bearings	21
9	Roller Weight and Skew Angle Wear Data	42
10	Multivariate Linear Regression for Roller Weight Change	43
11	Multivariate Linear Regression for Roller Skew Angle Change	44
12	Parametric Roller Bearing Experimental Wear Results	52

SUMMARY

The experimental program described herein was aimed at generating additional test data on a number of parametric roller bearings, and to correlate the results of these tests with the analytical model developed under NAPC Contract N00140-76-C-0383 and described in References 1 and 2.

During this program some of the most important roller bearing parameters, as identified previously during the NAPC and other P&WA programs, were evaluated over additional levels of variation. The results of this program, combined with the NAPC and P&WA programs, established the levels for optimum performance of those parameters having the most influence in effecting roller skewing or skidding and thus provided actual performance data for correlation with the bearing prediction analysis developed under the NAPC contract.

Six separate bearing designs were evaluated during this program. The six designs permitted the quantification of the influence of four important bearing parameters on roller skew and skid. Three of the parameters were evaluated at two levels of variation and the fourth parameter was evaluated at three levels. The six bearings each successfully completed the 10-hour parametric test, the same as that used during the NAPC program (Reference 1 and 2), up to speeds of 3.0 MDN. A wide range in the magnitude of roller end wear was obtained due to the number and magnitude of parameter variation levels evaluated. Analysis of the wear and other test data, however, revealed trends that were significantly useful for determining optimum parameter levels for future bearing designs.

SECTION I INTRODUCTION

BACKGROUND

The higher thrust-to-weight ratios required for advanced aircraft turbine engine designs demand increased rotational speed of the turbines and compressors. The design and development of such turbomachinery is often complicated by bearing considerations. The rotor and rotor support systems are generally characterized by high shaft speeds to achieve maximum gas dynamic performance, minimum size, and minimum weight; flexible bearing support structures for light weight and minimum disruption of the flowpath by interdiction of struts and vanes; and large shaft diameters for high bending and torsional stiffness. These factors result in bearing specifications which require high bearing DN levels and high misalignment capability. It is anticipated that speed levels to 3.0 MDN (million DN) will be required for engines in the 1980-1990 time frame.

Considerable effort has been expended by investigators on upgrading the performance of high DN ball thrust bearings, and this effort has produced many tens of thousands of hours of operating time at 3.0 MDN under laboratory conditions. Ball thrust bearing technology has evolved to where material considerations determine the life limits of the design. However, the technology base needed for the design of optimum roller bearings to meet high DN requirements is not well defined. In many cases, roller bearing performance has been the limiting factor in the design of high speed rotor systems because of a lack of understanding of certain aspects of roller bearing behavior. There is good reason for this. The increased susceptibility of roller bearings to fail has surfaced in relatively recent times. Ever increasing engine rotational speeds have driven bearings up to DN levels which serve to intensify the influence of geometric variations and other parameters on roller dynamics. Evidence accumulated in the field, and data obtained in development tests, indicate that bearing performance is very sensitive to roller instabilities.

These instabilities occur frequently in high DN bearings and cause roller skewing. The characteristic failure mode which identifies roller skew is rapid eccentric wear on the end surfaces of some or all of the rolling elements of a bearing. Figure 1 shows the eccentric wear pattern on one end of a roller, with the other end having a similar pattern but 180 degrees out of phase. This condition can exist undetected until bearing failure occurs. Figure 2 shows a typical example of bearing failure precipitated by eccentric end wear of one roller element.

Related to skewing, and apparently influenced by many of the same forces which induce it, is roller skidding. When rollers skid, the resulting damage is particularly severe on the rolling contact surfaces and, subsequently, has an adverse effect on bearing durability. Currently, skidding is considered to be of secondary importance compared to roller end wear. This conclusion is based upon considerable field service experience. Data indicate that roller end wear failures predominate. The mechanisms that cause skidding are more readily understood, and inherent in this understanding is the suggestion for its control. It is well known that roller skidding occurs when bearing radial loads are light and rotational speeds are high. A concept commonly used to supplement the external load is a two-point radial preload design. This basic preload system, which is achieved by machining the outer ring OD in an out-of-round oval shape combined with a slight interference fit in the bearing housing, adds enough load to keep the rollers "in gear" around most of the bearing's circumference. However, as speeds increase, the ability to maintain control of the internal clearance needed to ensure operation free of skidding damage becomes increasingly dependent upon accurate knowledge of the internal heat generated by the bearing. This factor, coupled with the cooling system design, determines the operating temperature level of the bearing and, more importantly, the temperature differential from the inner to the outer raceway. Thus, an accurate knowledge of the heat generated is a necessity if adequate control of operating clearance is to be achieved so that roller loading is maintained at a level that successfully inhibits roller skidding.



FD 184180

Figure 1. Eccentric Roller End Wear Due to Interaction With the Face of the Inner Ring Guide Flange



Figure 2. Typical Bearing Failure Attributable to Eccentric Roller End Wear

FD 184181

Of course, there are other modes of engine roller bearing failure besides those attributable to end wear and skidding. Some of these modes are identifiable with the cage and others may be due to roller edge loading causing premature fatigue spalling. However, it appears highly likely that if the basic roller end wear problem — as influenced by skewing action — can be avoided, a large measure of the solution to other root problems can be effected. This becomes largely self-evident upon study of the long list of geometric, dimensional, tolerance, quality, and operational parameters which influence and control roller tracking forces. A design system which provides identification and regulation of these factors will provide a means for establishing the entire bearing design. For these reasons, this system must go beyond a quasi-static analysis and must address roller bearing dynamic behavior.

PROGRAM APPROACH

Design Requirements

Future engine design requirements dictate roller bearing DN levels to 3.0M. Therefore, roller bearing technology to achieve this DN level must be upgraded in time for utilization in engines slated for operation in the 1980-1990 time frame. The schedule to develop bearings to meet the 3.0 MDN requirements calls for an extension of the present state-of-the-art of bearing design and requires considerable analytical and design effort to investigate the effects of increased DN levels on many critical design parameters. In addition to the conventional parameter studies, involving fatigue life, stresses, temperature, fits, clearances, alignment, lubrication, and rotor dynamic response, special attention must be given to roller skidding and skewing motion which have been identified as possible problem areas for high DN operation. Proper analysis of these effects requires development of a new computer program which considers the complete dynamic motion of each element in the roller assembly.

In 1975 a program was initiated at P&WA, under NAPC Contract N00140-76-C-0383, directed toward the formulation of a viable generalized roller bearing analytical system which considered a number of geometrical and operational parameters. This development program was based on an integrated analytical/experimental effort. The design system, in the form of a complete computer program, is intended to provide the bearing design engineer with a useful tool for studying the static as well as dynamic characteristics of high DN roller bearings for future aircraft engine mainshaft applications.

The design system will be useful in the conduct of analytical experiments under simulated operating conditions. A parametric study utilizing a reliable analytical design system could establish basic design criteria, help to separate the important variables from the unimportant ones, predict the effect of each controllable design factor and thus could substantially reduce the number of costly test programs in the early phase of new bearing development. It could also be used to assist in the diagnosis of roller bearing failures in service engines.

As previously summarized, References 1 and 2, the main obstacle to advancing high speed roller bearing technology is related to roller element skewing and skidding and the resultant wear and surface damage. Thirty bearing variables considered as having an influence on roller skew and skid have been identified, as shown in Table 1. Operational variables, such as bearing speed, externally applied load, and lubricant temperature were not counted in this total. The basic categories considered were design geometry, including internal lubrication arrangements, manufacturing tolerances, and quality control variables. As shown in Table 1, these 30 variables were divided into three categories. Category I includes 14 variables that are considered to have the greatest direct influence on the roller bearing wear phenomena normally identified as skidding damage and roller end wear of either the uniform and concentric type or of the uneven and eccentric type. Category II is composed of 8 variables considered to have less direct impact on wear and Category III is composed of 8 variables judged to have the least direct effect. The criteria employed in making these assessments, although somewhat subjective, were based, in large measure, on experience from experimental test results and from field service reports, in addition to analytical studies, manufacturing surveys, and an understanding of the physical phenomena affecting bearing behavior.

TABLE 1. RELATIVE RANKING OF ROLLER BEARING VARIABLES

<i>Roller Bearing Variable</i>	<i>Possible Effect of Variation</i>	<i>Rationale</i>
CATEGORY I:		
Roller Length/Diameter Ratio	Uneven roller end wear	Alters roller element gyroscopic action stability achieved by L/D ratio of 0.87.
Roller Unbalance (Nonhomogeneous material, roller end runout, crown radius runout)	Uneven roller end wear	Alters skewing forces as rollers impact guide flanges.
Preload	Controls skidding and can reduce damage on roller surfaces and raceway surfaces.	Roller element skids or slips "out of gear" due to insufficient loading.
Cage Unbalance	Local cage bore wear for inner land guided cage, end wear adjacent roller(s) and skidding damage.	Rub causes local overheating and decreases effectiveness of oil film.
Roller Flat Centrality	Uneven roller end wear	Alters tractive force profile of roller as well as stability about transverse axis due to unsymmetrical roller mass distribution.
Roller End Circular Runout	Uneven roller end wear	Affects roller stability about transverse axis and modifies roller end face contact stress.
Roller End Shape	Uneven and concentric roller end wear	Alters lubrication film and roller end contact stress.
Raceway Taper	Concentric roller end wear	Alters distribution of roller tractive forces.
Roller End Clearance	Uneven roller end wear	Alters maximum roller skewing angle thus changing end face contact forces.
Roller Diameter Variation	Uneven roller end wear/roller skid damage	Alters maximum roller skewing angle/alters roller tractive forces.
Lubrication	Uneven and concentric roller end wear, roller skid damage, cage wear	Alters effective oil film thickness.
Flange Height	Uneven and concentric roller end wear	Alters roller skewing angle and roller end contact stress and location.
Raceway Angular Misalignment	Concentric roller end wear/reduced fatigue life	Alters roller tractive forces and distribution/alters roller load profile.
Percent Flat Length of Roller	Fatigue life and uniform end wear	Alters roller load profile, tractive forces and skewing moment.
CATEGORY II:		
Roller Clamping Load	Concentric roller end wear	Reduction in roller end clearance due to guide flange deflection alters oil film thickness and roller end contact profile.
Flange Face Runout	Uneven roller end wear	Alters maximum roller skewing angle and dynamic end face loads.
Roller Crown Radius	Fatigue life and concentric roller end wear	Alters roller load profile, modifies tractive forces and skewing moments.
Extended Roller Flat Length	Fatigue life and uniform end wear	Alters roller load profile, tractive forces and skewing moment.
Flange Face Waviness	Uneven roller end wear	Alters maximum roller skewing angle and dynamic end face loads.

TABLE 1. RELATIVE RANKING OF ROLLER BEARING VARIABLES (Continued)

<i>Roller Bearing Variable</i>	<i>Possible Effect of Variation</i>	<i>Rationale</i>
CATEGORY II: (Continued)		
Flange Layback Angle	Uneven roller end wear/concentric roller end wear	Alters maximum roller skewing angle, oil film thickness and location of end face contact area.
Roller-Cage Pocket Clearance	Uneven roller end wear	Affects transmission of any cage instability altering roller-to-guide flange contact loads and tractive forces.
Flange Contour	Uneven roller end wear/concentric roller end wear	Alters maximum roller skewing angle, oil film thickness, and roller end contact area and location.
CATEGORY III:		
Roller Length Variation	Uneven roller end wear	Alters maximum roller skewing angle.
Cage Pocket Offset	Not apparent unless extreme, causing uneven roller end wear	Alters resultant skewing force of roller element.
Roller End Surface Finish	Uneven and concentric roller end wear	Alters oil film thickness requirements at roller ends.
Flange Surface Finish	Uneven and concentric roller end wear	Alters oil film thickness requirements at roller ends.
Raceway Surface Finish	Skid damage	Alters roller tractive forces and oil film thickness requirements at roller raceway contacts.
Cage Pocket Squareness	Concentric roller end wear	Alters resultant skewing force acting on roller element.
Raceway Waviness	Skid damage	Imposes dynamic loads on roller affecting variations in tractive forces and oil film thickness requirements at contacts.
Roller Taper	Uneven roller end wear	Alters tractive force profile of rollers as well as roller stability about transverse axis due to unsymmetrical mass distribution.

Under Contract N00140-76-C-0383, two groups of bearings were formulated using statistical design techniques. The first group, Group-N, consisted of eight separate bearing designs which allowed the influence of seven individual bearing parameters on roller skid and skew to be quantified. The second group, Group-AF, consisted of five bearing designs which allowed four additional parameters to be studied. In addition, under a Pratt & Whitney Aircraft sponsored program a third group of bearings, Group-P&WA, consisting of eight designs, permitted the evaluation of seven additional parameters.

The three groups of bearings, a total of 21 separate designs, were evaluated in a similar manner. The program included complete pre- and post-test inspection of all the bearings and their components in addition to experimental rig evaluation of each bearing at speed levels up to and including 3.0 MDN. The wear and performance obtained for the three groups of bearings were reduced and analyzed. Subsequently, the results were correlated with the roller bearing analytical model developed under Contract N00140-76-C-0383.

PROGRAM SCOPE

The work performed under the contract covered by this report was an effort to further evaluate the important roller bearing parameters affecting bearing performance, as determined from the results of the NAPC Contract N00140-76-C-0383 and other Pratt & Whitney Aircraft studies and experimental programs. This program was organized into two phases. In Phase I, the results obtained in the experimental evaluation of the Group-N bearings under the NAPC contract and from Pratt & Whitney Aircraft programs were reviewed. Four parameters that indicated a significant effect on roller bearing performance as determined by the operational and roller wear data were identified. Using these four parameters, six separate parametric bearing designs were prepared using the partial factorial designed experiment approach. This set of bearings has been assigned the designation Group-AF4. The same 124.3 mm basic bearing used in the design of the NAPC contract parametric bearings was again used as the basis for the design of the bearings for this program. These bearings were manufactured and tested so as to allow evaluation of the effect of at least two levels of the four selected parameters. These levels were in addition to the two levels investigated under the NAPC and P&WA programs. A total of 60 hours of testing was conducted on the six bearings.

In Phase II, the test data obtained in Phase I were compiled and reduced. Statistical techniques, such as regression analysis, were utilized to determine the influence of each parameter on high speed roller bearing performance. The results of experimental data analysis, which included both roller bearing operational and wear results, were correlated with the bearing prediction analytical model developed under the NAPC contract.

SECTION II

PARAMETRIC AND VERIFICATION TESTING — PHASE I

PARAMETER SELECTION

The selection of the bearing parameters for evaluation was based on the results obtained from the testing conducted under NAPC Contract N00140-76-C-0383, Air Force Aero Propulsion Laboratory MIPR FY 14557600623, and a separate Pratt & Whitney Aircraft program. The summary results from these three programs which identify the effects of the various parameters investigated on roller wear are presented in Table 2. Included in this presentation is identification of certain roller variables that were shown to have a significant effect on roller wear as indicated by weight loss and skew angle change results. It was further determined that roller coupled corner radius runout, which was evaluated in the NAPC Group-N bearings, had the most significant effect on roller wear. Of the eight bearings tested in this group, four contained rollers with a high level of coupled roller corner radius runout resulting in roller dynamic unbalance. The extremes of roller end wear occurring in these four bearings resulted in cage failure in each case.

Four other variables which were shown to have a significant, although confounded, effect on roller end wear are listed below:

Group-N

- Roller end circular runout
- Roller cylinder offset

Group-P&WA

- Roller end clearance
- Flange height

The results from testing the above two sets of variables were confounded because their level of variation was similar for each bearing in the two respective groups. Therefore, the individual effects of each of the two variables in each of the two groups could not be separated. On the basis of these results, the above four parameters were selected for further evaluation in this new program. This was done in a manner that allowed separation of effects and included additional levels of variation beyond those previously evaluated.

TABLE 2. ROLLER WEAR RESULTS FROM GROUP-N, GROUP-AF AND GROUP-P&WA TESTS

Variable	Levels Tested			Aug Roller Weight Change	Aug Roller Skew Angle Change
	Low	High	Baseline		
Group-N					
Preload	0	2 Point O.R.	2 Point O.R.	—	—
Roller Coupled Corner Radius Runout, in.	0.0008	0.005	0.0008	↓	↓
** Roller End Circular Runout, in. $\times 10^{-3}$	50	180	120	↓	—
Inner Race Taper, min	0.8	3.68	0.8	↓	—
** Roller Cylindrical Offset, in. $\times 10^{-3}$	10	50	10	↓	—
Raceway Misalignment, deg	0	0.5	0	—	—
Oil Flow, lb/min	13	29	20	—	—
Group-AF					
Extended Roller Flat, % Roller Length	48	67	40	—	—
IR Guide Flange Layback, min	15	60	15	—	—
IR Guide Flange Contour	Straight	Curved	Straight	—	—
IR Guide Flange Runout to Face, in. $\times 10^{-4}$	4	20	4	—	—
Group-P&WA Test					
Roller L/D Ratio, in./in.	0.77	1.0	1.0	↓	↓
Cage Unbalance, gm-cm	1.0	8.0	2.0	—	—
** Roller End Clearance, in. $\times 10^{-3}$	1	5	1	↓	↓
Roller End Shape, Max Protrusion, in. $\times 10^{-6}$	50	400	50	↓	↓
** Flange Height, % of Roller Dia	20	30	25	↓	↓
Roller Dia Variation, in. $\times 10^{-6}$	50	500	50	↓	↓
Roller Flat Length, % Roller Length	0	50	10	—	—
— No effect on output, either level or baseline value can be selected.					
↓ Trend with output is positive, select a lower level for minimum roller weight change and static skew angle change.					
↑ Trend with output to negative, select a higher level for minimum roller weight change and static skew angle change.					
* Indicates a significant roller bearing variable.					
** Results for these variables are confounded.					

DESIGN OF PARAMETRIC BEARINGS

The basic roller bearing selected for the design of the parametric bearings is shown in Figure 3. This bearing has a bore of 124.3 mm and is used in the No. 5 position of the TF30 model production engine. The parametric bearings evaluated earlier, and designated Group-N, Group-AF and Group-P&WA were also based on this same TF30 bearing design.

Six designs incorporating the four study parameters in the new Group-AF4 bearings were prepared for evaluation under Phase I of this program. The matrix shown in Table 3 describes the parameters varied for each of the six bearings, and indicates their relative magnitude by the symbols L, M, and H for low, medium and high. The actual magnitudes of the parameters being investigated in each of the six test bearings are compared with those of the baseline bearing in the table shown in Figure 4. The specific magnitudes chosen were established on the basis of analytical, manufacturing and production experience, and to a large degree by a desire to be consistent with the levels previously evaluated during the NAPC, Aero Propulsion Laboratory and P&WA experimental programs.

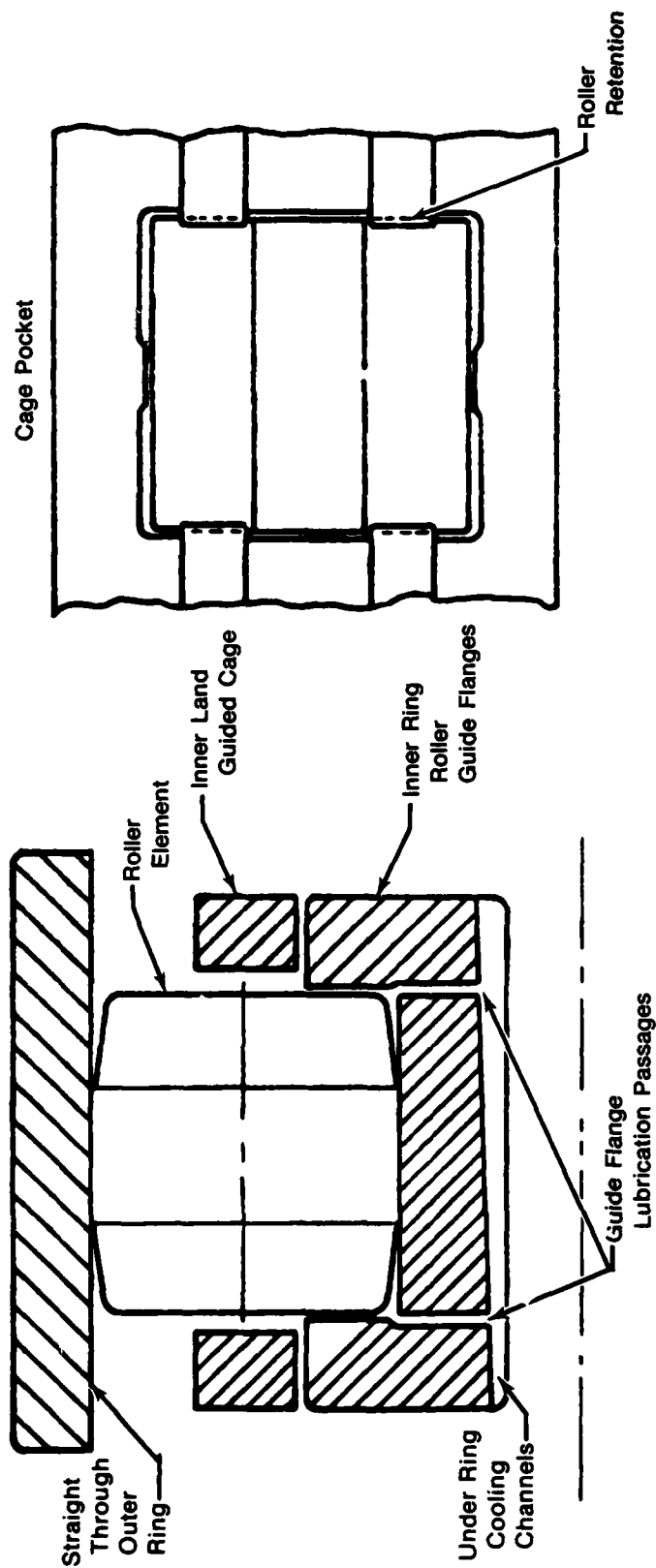
All parameters which were not studied in this program were maintained at the levels used in the basic bearing except for the outer ring out-of-round, which is used to provide an internal load, or preload, which comes about from the resulting diametral "pinch." The out-of-round selected should provide a preload at the operating condition of concern sufficient to control skidding and allow the roller complement to orbit at kinematic angular velocity. Excessive out-of-round on the other hand, results in a stress condition which can further aggravate the situation. An inner ring stress level that is too high could result in inner ring fracture. Inner ring fractures experienced during previous high speed running, Reference 2, may have been caused, at least in part, by high preload levels. The preload for the six Group-AF4 bearings was reduced accordingly.

TABLE 3. MATRIX USED IN THE DESIGN GROUP-AF4 PARAMETRIC ROLLER BEARINGS

6 Roller Bearing Designs
4 Bearing Variables
2 or 3 Levels of Variation

- L - Low
- M - Medium
- H - High

Roller End Clearance	Flange Height	L		H		Roller End Circular Runout	Roller Flat Centrality
		L	H	L	H		
L	L		Bearing No. 27				
	H			Bearing No. 28			
M	L					Bearing No. 29	
	H		Bearing No. 30				
H	L	Bearing No. 31					
	H					Bearing No. 32	

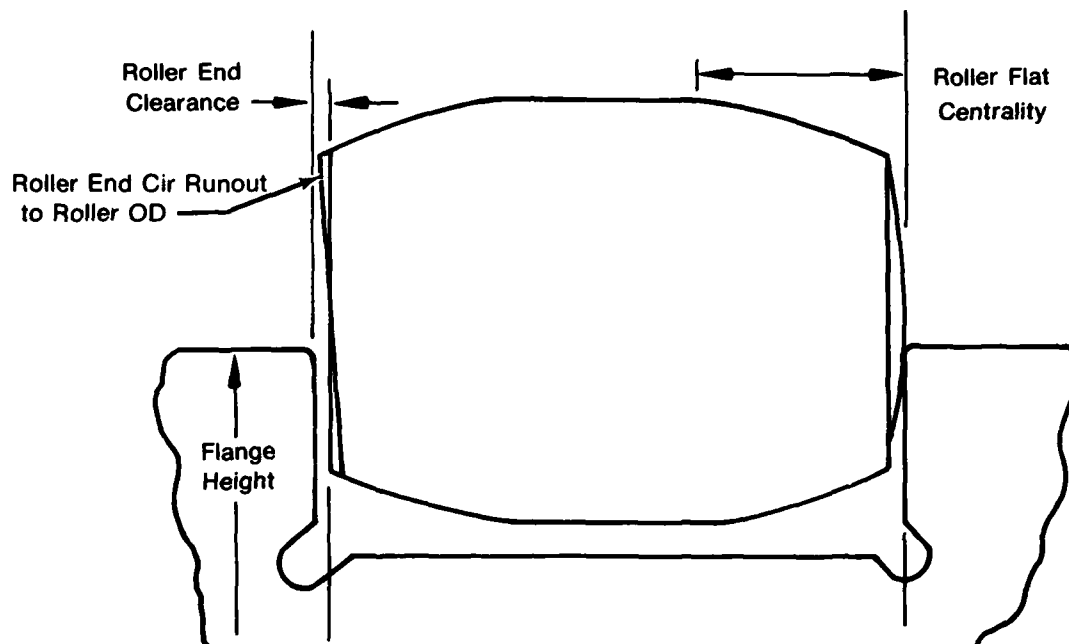


Cage Material : AMS-6414
Cage Plating : Silver per AMS-2412

Inner Ring Bore Dia: 124.3mm
Basic Roller Size, L x D : 13 mm x 13 mm
No. of Rollers : 28
No. of Radial Lube Holes : 3 per Side
Bearing Material : VIM-VAR M-50

FD 104102

Figure 3. Basic Bearing for Parametric and Verification Testing



Bearing Number	Parameters			
	Roller End Circular Runout to Roller Outer Diameter, in.	Roller Flat Centrality, in.	Roller End Clearance, in.	Flange Height, % Roller Dia.
Baseline	0.00012	0.010	0.001	25
27	0.000050	0.050	0.001	20
28	0.000180	0.010	0.001	30
29	0.000180	0.050	0.002	20
30	0.000050	0.050	0.002	30
31	0.000050	0.010	0.005	20
32	0.000180	0.050	0.005	30

FD 184183

Figure 4. Parametric Roller Bearing Designs to Obtain Wear Data on Four Bearing Variables

A new out-of-round level of 0.006-0.008 inches was calculated using the computer program STATIC developed under the previously mentioned NAPC contract. This reduced level was chosen in order to provide a reduced bearing preload arbitrarily selected at 300 lbf. The ring temperatures required for the analysis were obtained from testing carried out under the same NAPC contract on bearings having a higher preload due to an out-of-round of 0.020-0.022 inch.

PROCUREMENT OF BEARING HARDWARE

The bearing manufacturer selected to fabricate the parametric bearings was the Split Ballbearing Co. (SBB), Division of MPB Corporation. SBB is a producer of the basic No. 5 mainshaft position roller bearing used in production TF30 engines. In addition, SBB has supplied experimental hardware of the 124.3 mm bearing size which has been evaluated in baseline tests to speeds of 3.0 MDN. SBB also supplied the parametric bearings evaluated under the NAPC, Aero Propulsion Laboratory MIPR, and P&WA programs as described in References 1 and 2. Thus, the refinement of the important roller bearing parameters was not subjected to the possible deleterious influence of alternate processing and inspection techniques that might have been encountered if another manufacturer was utilized.

One of each of the six parametric roller bearing designs was fabricated for experimental rig evaluation. Detailed inspection documentation of the components as well as of the six bearing assemblies was made and recorded by SBB. The specific geometry and tolerance features that were documented were the same as those recorded for the NAPC contract and Aero Propulsion Laboratory MIPR bearings. Some of the specific measurements that were provided by SBB are:

- Dimensions on at least four rollers (all rollers being serialized to facilitate identification) — length, diameter, corner radius runout, crown radius, length of central cylindrical section, flatness of central cylindrical section, offset of central cylindrical section, roller end circular runout, and crown drop.
- Diameters of the inner and outer rings
- Inner and outer raceway eccentricity and axial taper
- Roller guide shoulder face parallelism
- Roller guide flange angle
- Unmounted internal radial clearance
- Cage land clearance
- Surface finish of rollers, raceway and face of guide shoulders
- Cage unbalance
- Roller-to-guide flange clearance.

The inspection data which accompanied each of the six bearings were reviewed and no significant deviation was uncovered. Since up to 31 pages of inspection results were provided for each bearing, the inclusion of a complete compilation of this data in this report would be unrealistic. However, a summary of these inspection results has been provided in Table 4 with average measurements shown where possible.

**TABLE 4. SUMMARY OF VENDOR MANUFACTURING INSPECTION DATA FOR
GROUP-AF4 ROLLER BEARINGS**
(Measurements in inches unless otherwise designated)

	Bearing Number						
	Baseline	27	28	29	30	31	32
<i>Bearing Assy</i>							
1. Cage Clearance	0.0176	0.0190	0.0190	0.0180	0.0180	0.0190	0.0190
2. Roller End Clearance	0.0012	0.0010	0.0009	0.0018	0.0019	0.0052	0.0052
3. IRC (Unmounted)	0.0040	0.0040	0.0042	0.0042	0.0042	0.0044	0.0039
<i>Rollers</i>							
1. Length	0.51175	0.51187	0.51097	0.51180	0.51174	0.51178	0.51178
2. Diameter	0.51166	0.51180	0.51177	0.51182	0.51178	0.51161	0.51180
3. Surface Finish (AA)	—	3.0	3.0	3.0	2.5	4.5	2.3
4. Coupled Corner Radius Runout	0.001	0.0001	0.0001	0.0004	0.0001	0.0001	0.0003
5. Crown Radius	24	24	24	24	24	24	24
6. Cylinder Length	0.207	0.2015	0.2535	0.1870	0.178	0.2605	0.1970
7. Cylinder Flatness ($\times 10^{-6}$)	—	13	12	12	12	25	17
8. Cylinder Off-Set	0.010	0.044	0.004	0.044	0.048	0.006	0.050
9. End Circular Runout ($\times 10^{-6}$)	120	35	185	180	58	87	180
10. Crown Drop	0.00085	0.00077	0.00088	0.00077	0.00079	0.00080	0.00085
11. Hardness (Rc)	60 min	63.0	61.5	62.3	62.0	61.5	62.0
<i>Outer Ring</i>							
1. OD Max	6.7561	6.7486	6.7491	6.7488	6.7489	6.7490	6.7490
2. OD Min	6.7350	6.7419	6.7427	6.7424	6.7415	6.7424	6.7422
3. OD Avg	6.7456	6.7452	6.7459	6.7456	6.7452	6.7457	6.7456
4. ID	6.4246	6.4253	6.4256	6.4258	6.4255	6.4233	6.4254
5. Eccentricity ($\times 10^{-6}$)	25	38	30	20	50	50	38
6. ID Flatness ($\times 10^{-6}$)	15	22	29	27	23	6	12
7. Surface Finish (AA)	4.0	4.2	4.5	4.5	4.3	3.0	4.8
8. Hardness (Rc)	62.0	62.6	62.0	61.3	61.5	64.0	62.3
<i>Inner Ring</i>							
1. Bore Dia	4.8936	4.8937	4.8936	4.8937	4.8937	4.8936	4.8937
2. OD Overall	5.6773	5.6060	5.7075	5.6063	5.7074	5.6062	5.7073
3. OD Roller Path	5.3966	5.3973	5.3973	5.3975	5.3975	5.3972	5.3973
4. Roller Path Eccentricity ($\times 10^{-6}$)	18	18	10	13	10	12	10
5. Roller Path Taper	0	0	0	0	0	0	0
6. Guide Flange Angle (minutes)	6	4.0	4.1	5.1	4.3	4.3	4.4
7. Guide Flange Finish (AA)	4.90	3.75	5.75	3.75	5.00	5.75	5.00
8. Roller Path Finish (AA)	3.00	3.00	4.30	3.33	4.00	4.00	4.00
9. Hardness (Rc)	63.0	62.6	63.2	63.0	63.3	60.3	63.0
<i>Cage</i>							
1. ID	5.6977	5.6263	5.7252	5.6255	5.7249	5.6279	5.7249
2. Pocket Squareness ($\times 10^{-6}$)	450	500	750	550	450	500	550
3. Pocket Parallelism	0.0011	0.0017	0.0016	0.0012	0.0016	0.0011	0.0017
4. Unbalance (gm-cm)	1.32	2.86	0.36	0.57	2.50	2.43	0.93
5. Hardness (Rc)	33.0	36.0	37.7	37.0	35.7	36.7	36.0

PRETEST PREPARATION AND INSPECTION OF TEST BEARINGS

Preparation of all the bearings for test was completed. Each bearing outer ring was instrumented with a strain gage on the outer diameter surface to permit measurement of roller pass frequency during test. Thus, for each of the program test points it could then be determined whether or not the roller elements were skidding. Pretest preparation also included the weighing of each roller. Repeating this weighing process after the test permits determination of the amount of roller mass loss attributable to wear. For this measurement, a laboratory Christian Becker TORBAL Scale, Model EA-1, was used. Also, before and after test each of the rollers was measured for static skew angle of turn allowed by the inner raceway guide flanges. The pretest roller weight and static skew angle measurements obtained for the program bearings are found in Table 5.

TABLE 5. PARAMETRIC ROLLER BEARINGS — PRETEST WEAR RELATED MEASUREMENTS

<i>Bearing No.</i>	<i>Average Roller Weight, Grams</i>	<i>Average Roller Skew Angle, Minutes</i>
27	13.3841	15.46
28	13.3694	11.03
29	13.4000	23.52
30	13.3792	19.74
31	13.3850	58.07
32	13.3989	47.33

In addition to the bearing manufacturer's pretest inspection data, in-house measurements were made and recorded during installation of the bearings into the test rig. These measurements included the fits of the inner ring on the shaft and the outer ring in the support housing, the installed internal radial clearance of the test bearing and the angular misalignment of the installed outer ring. A tabulation of the measurements obtained for the six test bearings is shown in Table 6.

TABLE 6. PARAMETRIC ROLLER BEARING PRETEST RIG RELATED INSPECTION MEASUREMENTS

	<i>Bearing Number</i>					
	<i>27</i>	<i>28</i>	<i>29</i>	<i>30</i>	<i>31</i>	<i>32</i>
Inner Ring Fit on Shaft, Inch	0.0017T	0.0019T	0.0018T	0.0017T	0.0018T	0.0019T
Internal Radial Clearance Installed, Inch						
Minimum	0.0013	0.0006	0.0017	0.0008	0.0026	0.0006
Maximum	0.0044	0.0031	0.0047	0.0043	0.0050	0.0041
Average	0.0029	0.0019	0.0032	0.0026	0.0038	0.0023
Outer Ring Fit in Housing, Inch	0.0013L	0.0005L	0.0007L	0.0012L	0.0006L	0.0009L
Outer Ring Misalignment, Minutes	0	0	0	0	0	0

ROLLER BEARING TEST RIG AND INSTRUMENTATION

The test rig shown in Figure 5 was used for the experimental evaluation of the parametric bearings. It was originally designed and fabricated specifically for development testing of 115 and 124.3 mm bore diameter cylindrical roller bearings. Relatively trouble free operation has been experienced with this rig in the more than 5000 hours of testing accumulated to date, of which over 400 hours were at speeds of 3.0 MDN.

The test rig consists of a cylindrical housing, with a hydraulic load cylinder located centrally on top of the housing to apply a radial load to the test bearing. Three bearings are located on a common shaft assembly in the rig. The two bearings nearest the ends of the shaft assembly are rigidly bolted to the housing. The center or test bearing is mounted in a carrier attached to the load cylinder piston and is radially guided by tracks in the housing.

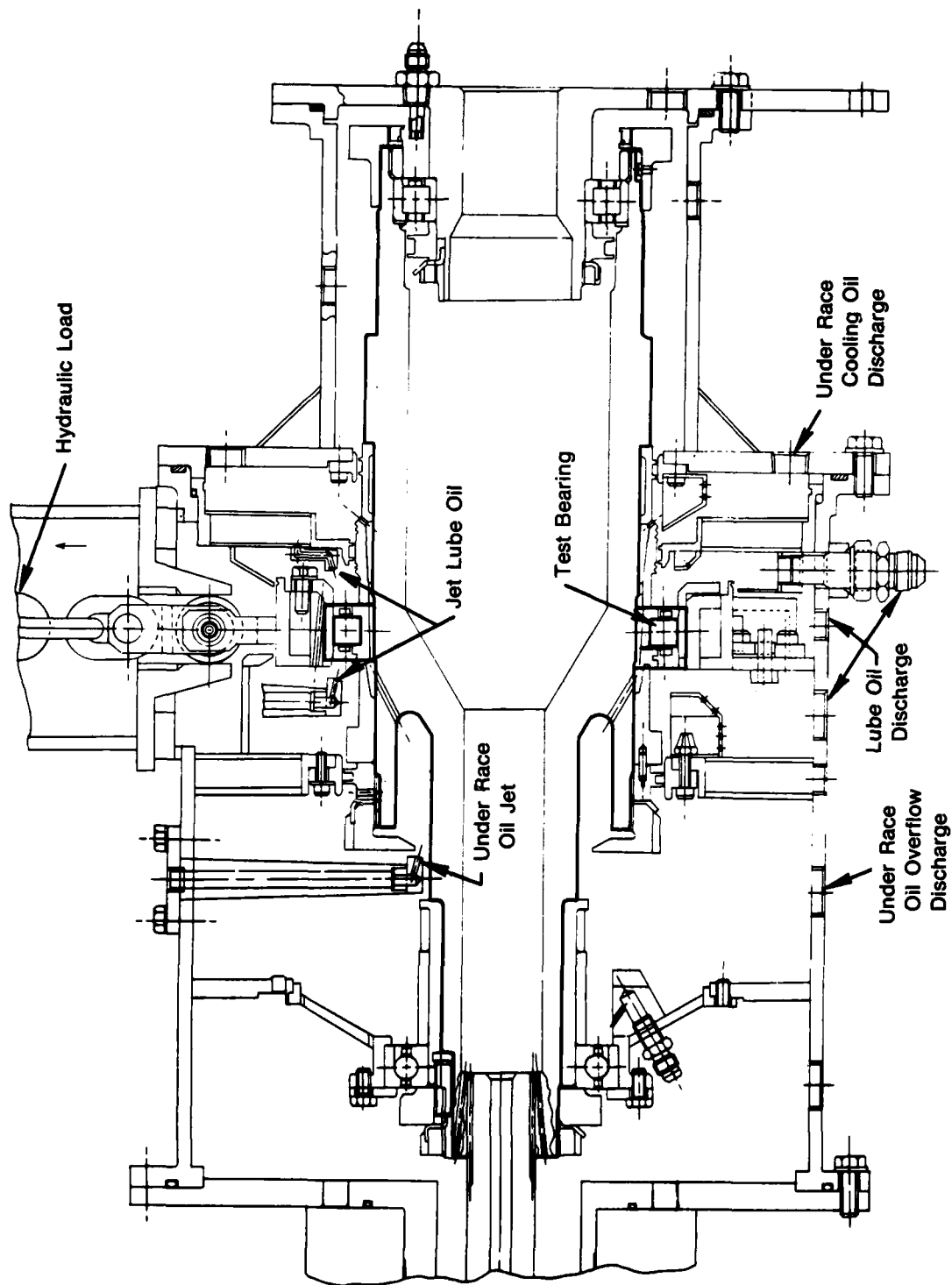
Radial load, applied to the test bearing by the load cylinder, is transmitted through the shaft assembly to the end bearings and then through the end bearing carriers to the housing. These bearings are equally spaced from the center bearing and each carries half the load applied to the center bearing. This arrangement maximizes alignment control among the bearings. Axial location of the shaft assembly is controlled by the ball thrust bearing mounted at the drive end.

Lubrication and cooling oil is supplied to the test bearing by directing jet oiling into both sides of the bearing cavity. Oil is also supplied separately from one side of the bearing in axial slots located under the rotating inner ring. Radial holdes intercepting a number of axial slots direct lubrication to the inner race roller guide flanges.

The test rig itself is serviced by the lubrication system shown schematically in Figure 6. This system provides the following functions:

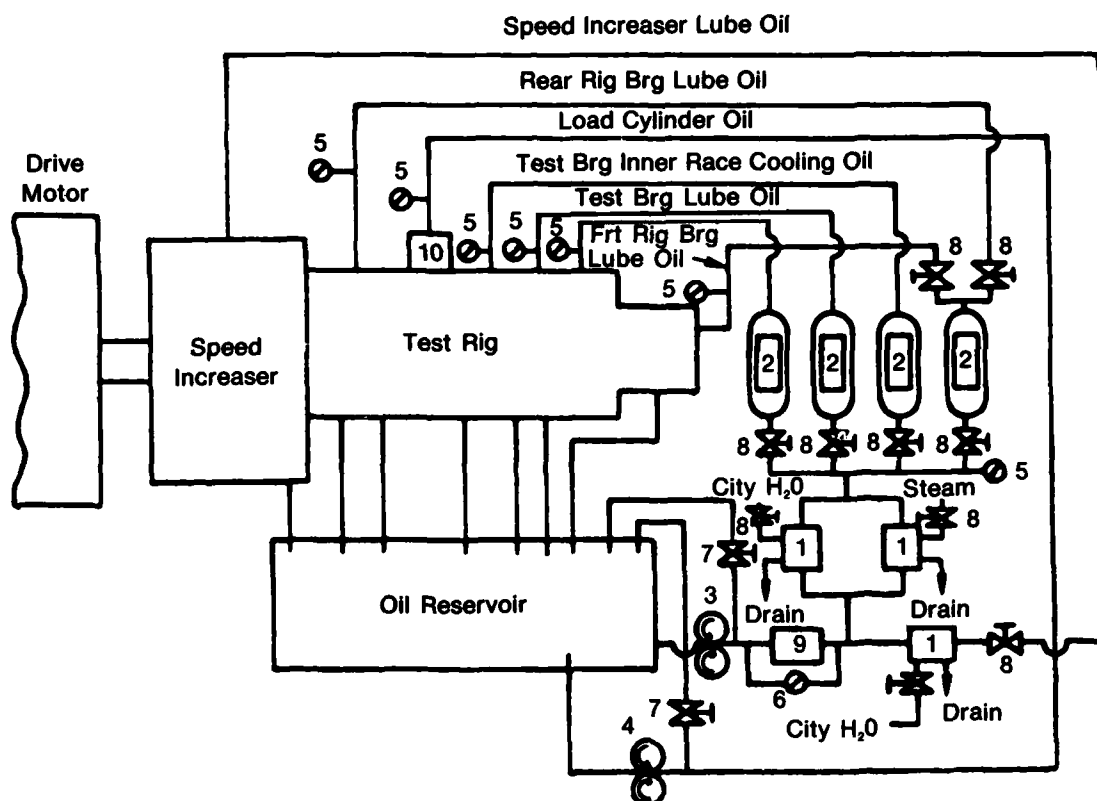
- Supplies oil to the test bearing as well as the rig slave bearings for lubrication and temperature control.
- Supplies oil to the speed increaser gearbox for lubrication of the gearbox bearings and gears.
- Supplies pressurizing oil to the hydraulic load cylinder of the rig to radially load the test bearing.
- Controls and monitors the temperature, pressure and flow of oil supplied to each part of the system.

The lubrication system includes an oil reservoir which supplies oil to two pressure pumps, one of high capacity and one of low capacity. The high capacity pump supplies oil to the test rig internals and to the gearbox. The low capacity pump supplies oil to the load cylinder which provides the radial load to the test bearing. The temperature of the oil to the test rig is controlled by a heat exchanger utilizing either high pressure steam for heating or water for cooling. Three delivery branches supply oil to the test bearing. Two of the branches supply the bearing with primary lubrication and provide outer race temperature control. The third branch supplies oil to the test bearing for both inner race temperature control and lubrication of the inner race guide flanges.



FD 194873

Figure 5. High Speed Roller Bearing Test Rig



1. Heat Exchanger
2. Flowmeter
3. High Volume Pressure Pump
4. Low Volume Pressure Pump
5. Pressure Gage

6. Pressure Differential Gage
7. Pressure Control Valve
8. Flow Control Valve
9. Static Filter
10. Hydraulic Load Cylinder

FD 184184

Figure 6. Lubrication System for Test Rig

Instrumentation is provided to measure the imposed test conditions, the bearing operating conditions, and the operating conditions of the test rig. This instrumentation consists of conventional devices which are maintained by the Contractor. Table 7 lists the measurement obtained and identifies the corresponding type of instrumentation employed. Manual recordings of all measurements are made every ten minutes during the calibration portion of the experimental program. During the endurance test portion of the program recordings are made once every twenty minutes.

TABLE 7. TEST INSTRUMENTATION

<i>Measurement</i>	<i>Instrumentation</i>
<i>Imposed Test Conditions:</i>	
Rig shaft speed	Tachometer generator signal from input to 7:1 ratio speed increaser, with tachometer readout.
Applied radial load	Pressure tap at hydraulic load cylinder supply port, with pressure gage readout.
Oil flow to test bearing	Magnetic type oil flowmeters with direct readout, installed in oil supply lines. Pressure taps in oil supply lines with pressure gage readouts.
Oil supply temperature	Chromel-alumel thermocouples installed in oil supply lines, with potential type readout.
<i>Test Bearing Operating Conditions:</i>	
Cage speed or slip	Strain gage cemented to OD of outer ring, with digital readout.
Outer ring temperature	Chromel-alumel thermocouples installed in housing, contacting bearing outer ring, with potential type readout.
Inner ring temperature	Chromel-alumel thermocouples installed in shaft, contacting bearing inner ring, with potential type readout via slip-ring.
Discharge oil temperature	Chromel-alumel thermocouples installed in discharge oil rig sumps, with potential type readout.
Horsepower and torque	Direct reading voltmeter and current indicating digital voltmeter.
<i>Rig Operating Conditions:</i>	
Rig bearing temperatures	Chromel-alumel thermocouples installed in housing, contacting bearing outer rings, with potential type readout.
Oil flow to rig bearings	Magnetic type flowmeters with direct readout, installed in oil supply lines. Pressure taps in oil supply lines with pressure gage readouts.
Vibration	Accelerometers (ENDEVCO, 2233E) mounted in vertical and horizontal plane on test rig, with vibration displacement meter readout.

EXPERIMENTAL PROGRAM PLAN

The test program followed during the rig evaluation of the Group-AF4 parametric bearings is similar to that employed under NAPC Contract N00140-76-C-0383 and Aero Propulsion Laboratory MIPR CY 14557600623. The program as shown in Table 8 was designed to obtain both calibration and endurance test data for each of the bearings. The calibration section consists of thirty separate test combinations designed to obtain bearing operational data with variations of speed, oil flow, radial load, and oil temperature. The imposed conditions were maintained at each test combination for ten minutes. From the operational test data obtained, the following performance parameters were determined:

- Heat generation
- Horsepower and torque
- Roller skid
- Inner and outer ring thermal stability
- Outer to inner ring thermal differential
- Axial and circumferential thermal gradients

Once the calibration portion of the ten-hour program was completed, endurance testing was conducted for the purpose of assessing the extended operating performance and roller wear durability of each bearing design. A portion of the endurance testing was conducted at the 3.0 MDN steady-state condition noted in Table 8. For the remainder of the endurance testing, the bearing speed was cycled between the two speed levels indicated in Table 8. A total of 30 acceleration-deceleration cycles were completed on each bearing. This simulates the type of transient operation found in gas turbine engines where increased bearing wear due to skidding and skewing may be encountered due to the rapid accelerations experienced by the roller elements.

TABLE 8. THE TEST PROGRAM PROVIDES FOR THE THERMAL PERFORMANCE AND SHORT TERM WEAR ASSESSMENT OF THE PARAMETRIC ROLLER BEARINGS

	Supply Oil				Bearing Load,lbf	Bearing DN/Test Point No.						Test Hr
	lb/min					1.0	2.0	2.5	2.75	2.9	3.0	
	Under Ring	Per Side Jet*	Total	°F								
Calibration	10	5	20	225	250	1	4	7	10	13	16	3
					500	2	5	8	11	14	17	
					1000	3	6	9	12	15	18	
	5	4	13	225	500	19	20	21	22	23	24	1
	11	9	29	275	500	25	26	27	28	29	30	1
Steady-State	10	5	20	225	500	Endurance at 3.0 MDN						4
Cyclic Speed	10	5	20	225	250	2.0 - 2.75 MDN Accels-Decels						1

*Two jets, one directed at each side of bearing

At the completion of each test, the experimental data were reduced to obtain the individual performance parameters. In addition, the overall condition of each bearing was noted and any distress or unusual wear was photographed. Each roller element was weighed and also measured for the static angle of turn allowed within the inner ring guide flanges. Using the pretest and post-test measurements, roller wear as determined by weight loss, and roller and guide flange wear as determined by change in static skew angle was determined. Each bearing was then ranked on the basis of wear. Using statistical regression analysis techniques the bearing parameters within each group were also ranked on the basis of relative wear.

BEARING PARAMETRIC TESTS

All six experimental bearings, designed and procured under Phase I of this program, completed the 10-hour rig test outlined in Table 8. Although stable operation was observed during each test, a wide range of wear and performance was obtained.

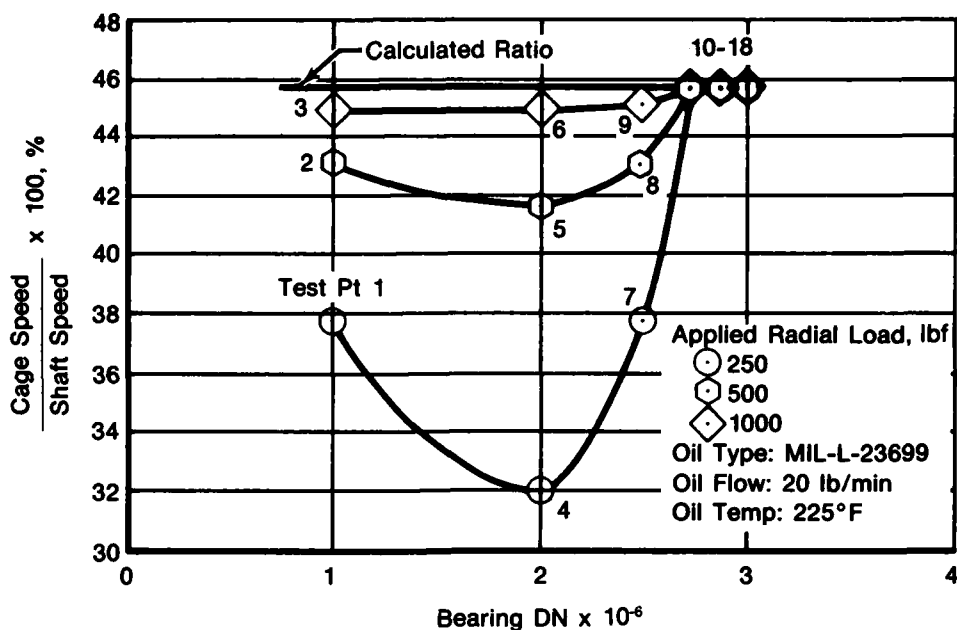
Experimental Evaluation of Parametric Bearing No. 31

Bearing No. 31 was the first of the group to be received from the manufacturer. After the necessary pretest inspection and preparation, the bearing was installed in the test rig for experimental evaluation. Testing of the bearing proceeded as outlined in Table 8. Roller pass frequency measurements indicated that roller skid was occurring in the speed range of 1.0 to 2.5 MDN. At speeds of 2.75 MDN and above, the rollers did not skid, as indicated by the frequency measurements. The magnitude of the skid, as shown in Figure 7, was the greatest at 2.0 MDN, with the maximum amount of skid occurring at the lowest applied radial load. Stable operation of the bearing was noted throughout the steady state endurance portion of the test.

Figure 8 shows the outer-to-inner ring temperature differential as a function of speed with variations in oil flow. The temperature differentials were not significantly affected by variations in radial load. Therefore, to retain clarity in the data presentation, only the results from the 500 lbf load run are shown in Figure 8. As indicated, oil flow variation had a pronounced effect on the inner-to-outer ring temperature differential for bearing No. 31. Data for the temperature differential during the 29 lb/min oil flow test was not obtained because the slip ring, which is required for obtaining inner ring temperature measurements, failed at 3.0 MDN during the 13.4 lb/min oil flow testing.

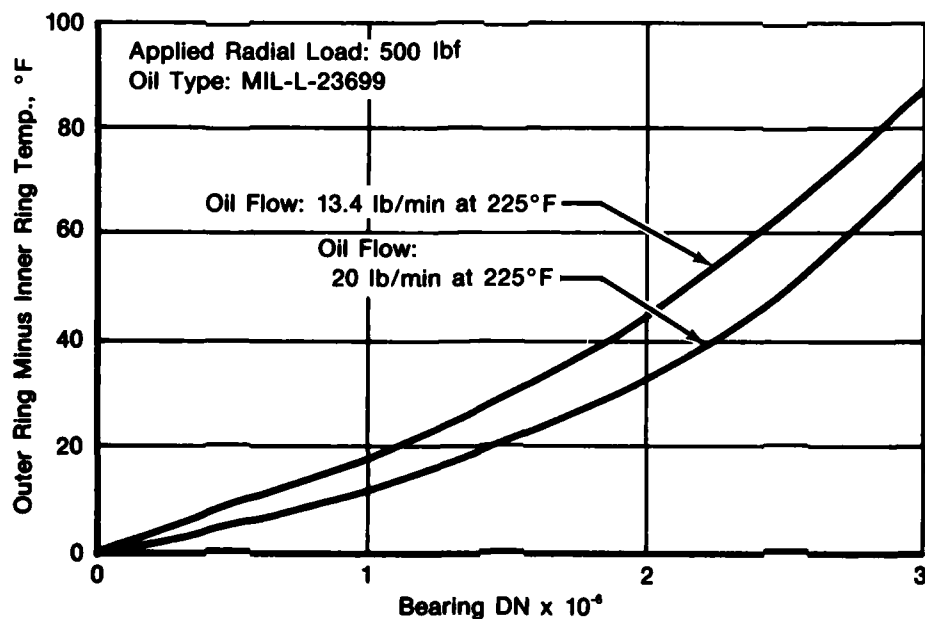
In Figure 9 it can be seen that DN level has a significant impact on heat generation. It is also apparent that increasing oil flow also causes a considerable increase in bearing energy consumption. Since the effect of radial load variation on heat generation was slight, only the 500 lbf results are shown in order to minimize clutter in the figure. Outer ring temperature less oil-in temperature as a function of bearing speed is shown in Figure 10. Varying oil flow, as can be seen in this figure, has a significant impact on the temperature differential.

Post-test inspection of bearing No. 31 proved it to be in generally good condition. Heavy concentric wear was observed on the ends of all the rollers and it was determined that the roller weight loss averaged 0.0061 grams while the roller skew angle increased an average of 32.43 minutes. These wear values when compared to those reported in Reference 2 for the Group N and AF testing fall toward the middle of the range. No distress or unusual wear patterns were noted on any of the other bearing components. Although roller skidding was indicated during test, no skid damage to either the roller elements or the raceways was apparent. The post-test condition of the bearing components can be seen in Figure 11 where concentric roller end wear can be seen.



FD 184185

Figure 7. Cage Slip of Bearing No. 31 Decreases as Applied Load Is Increased With No Skid Observed at Speeds Above 2.75 MDN



FD 184186

Figure 8. Outer to Inner Ring Temperature Differential for Bearing No. 31 Increases with Reduced Oil Supply

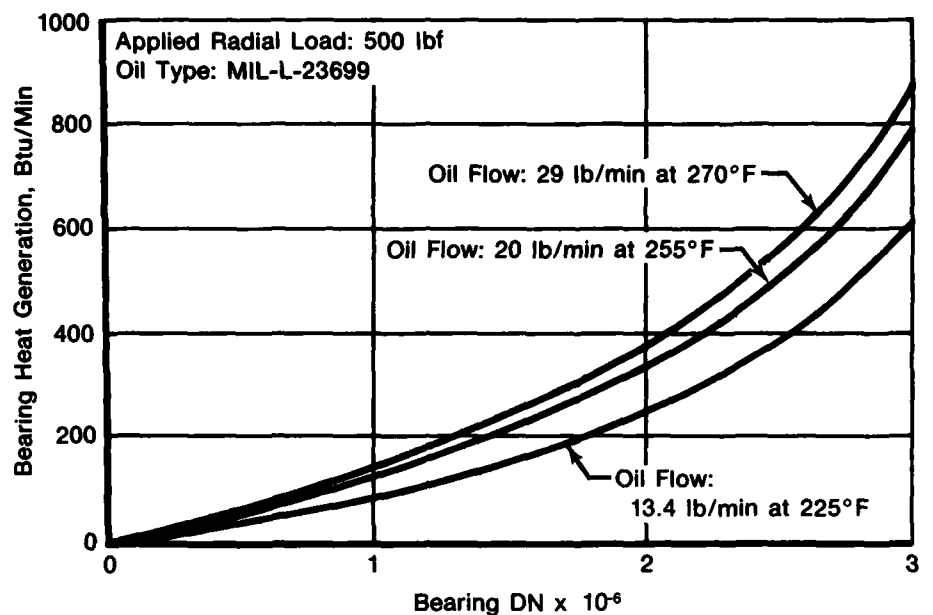


Figure 9. Increasing Oil Flow Results in Increased Heat Generation of Bearing No. 31

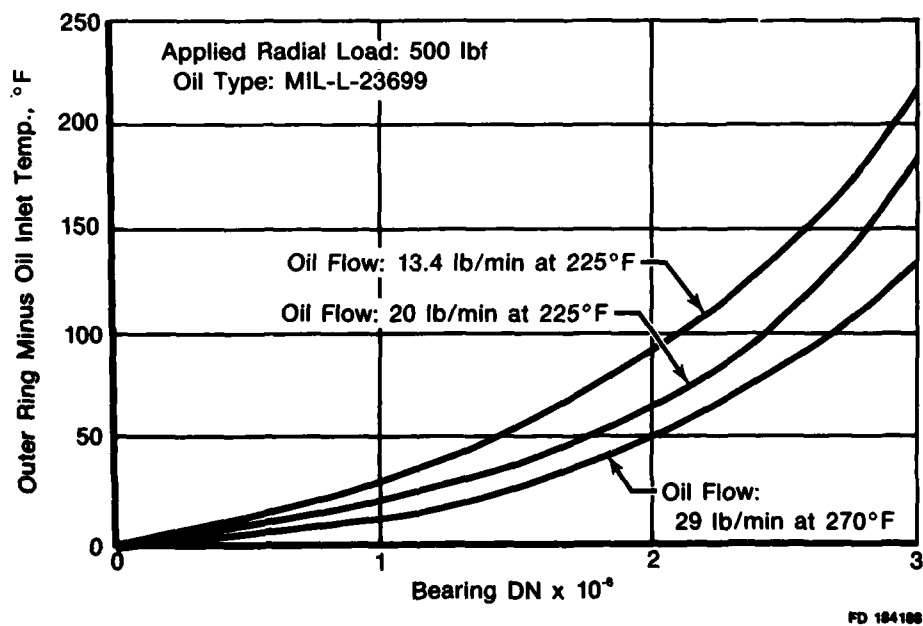
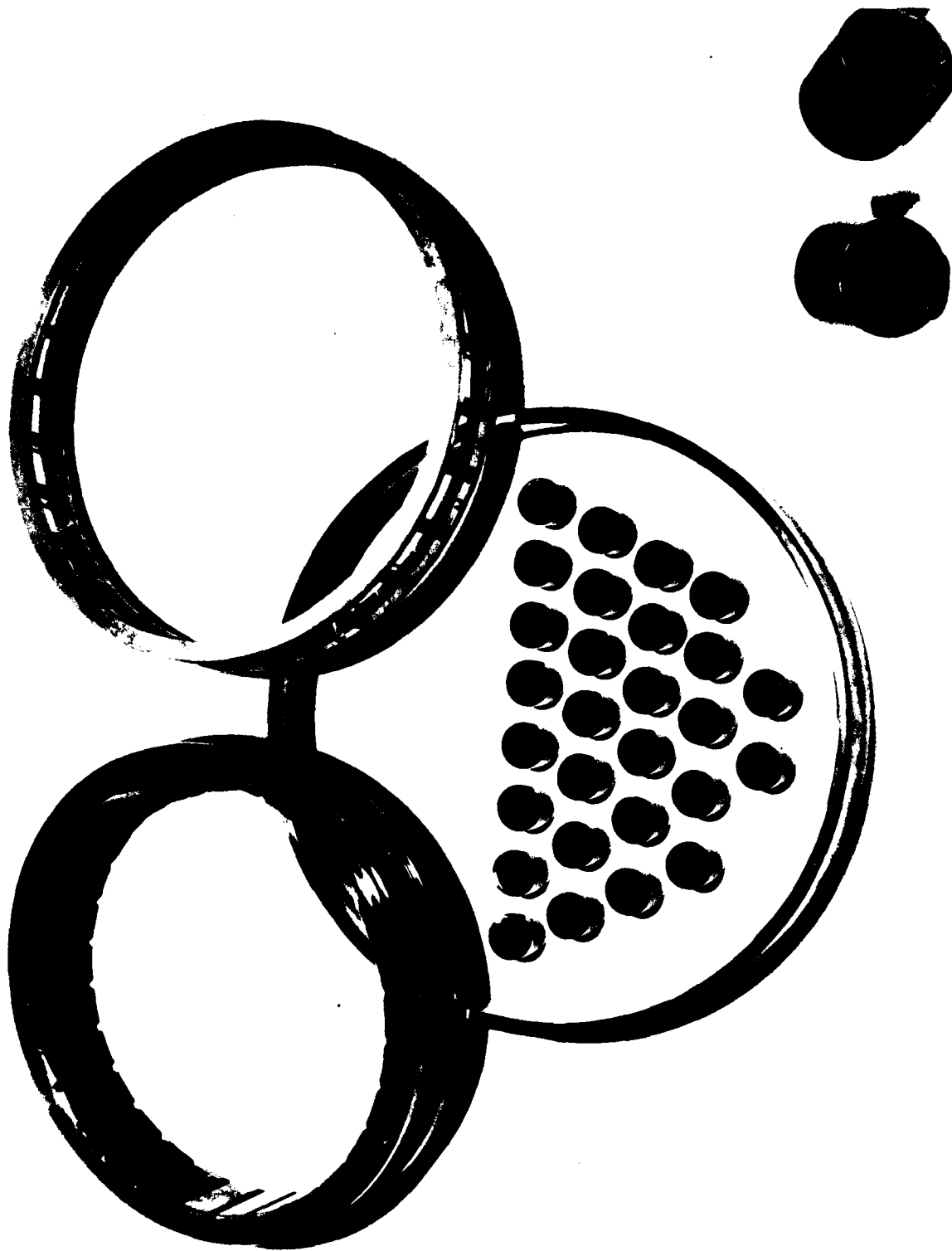


Figure 10. Bearing No. 31 Demonstrates that Increasing Oil Flow Results in Reduced Outer Ring-to-Oil Inlet Temperature Differential



FD 163257

Figure 11. Concentric Roller End Wear Can Be Observed in Parametric Bearing No. 31. No Skid Damage Was Apparent

Experimental Evaluation of Parametric Bearing No. 27

Parametric bearing No. 27 was the second design to be experimentally evaluated. As shown in Figure 4, this design included a high level of roller flat centrality, and low levels of flange height, roller end circular runout and roller end clearance. After installation of the bearing in the test rig, the 10-hour test described in Table 8 was initiated. While running at test point No. 17, a sudden, loud noise occurred with no increase in rig vibration noted. Testing was interrupted to investigate the cause of the noise with the rig subsequently disassembled for removal of the test bearing. Visual inspection of bearing No. 27, as well as the remainder of the rig components, proved them all to be in good condition with no signs of unusual wear or distress. The rollers were found to have light amounts of eccentric and concentric end wear. At this time the roller elements were weighed and measured for skew angle as well as dimensionally inspected for both corner radius and end run out. The results tabulated below indicate no significant wear had occurred to either the rollers or inner ring guide flanges. This study of the bearing and the rest of the test rig and drive system failed to reveal the source of the noise.

	<i>Pretest</i>	<i>After 3 hr of Test</i>	<i>Change</i>
Avg Roller Weight, gm	13.3842	13.3821	0.0021
Avg Roller Skew Angle, min	15.46	24.38	8.92
Avg Roller Coupled Corner Radius Run Out, in.	0.0001	0.0001	0
Avg Roller End Circular Run Out, in.	0.00035	0.00036	0

Parametric bearing No. 27 was then re-installed in the rig and the remainder of the 10 hour test was completed without incident. Examination of the bearing after test proved it to be in good condition with no indication of severe wear or distress as seen in Figure 12. The roller end wear patterns were in general concentric with several rollers exhibiting very slight eccentric wear. As shown below very little additional wear occurred during the last seven hours of test.

	<i>After 3 hr</i>	<i>After 10 hr</i>
Avg Roller Weight Loss, gm	0.0021	0.0022
Avg Roller Skew Angle Increase, min	8.92	9.86

Roller pass frequency measurements for bearing No. 27 indicated that the rollers were skidding in the speed range of 1.0 to 2.75 MDN. As seen in Figure 13, the degree of roller skid at 2.75 was less than 0.5% at all radial test loads, and no skidding was occurring at 2.9 or 3.0 MDN. The magnitude of skidding was the greatest at 2.0 MDN, with the maximum amount occurring with the lowest radial load of 250 lbf. Stable operation of the bearing was noted throughout the four hours of steady state endurance testing which was performed at 3.0 MDN.

Thermal performance results for bearing No. 27, Figures 14 and 15, indicate that decreased oil flow reduces heat generation while increasing the outer ring-to-oil inlet temperature differential. These are similar to the results shown for the previous bearing tested, No. 31.

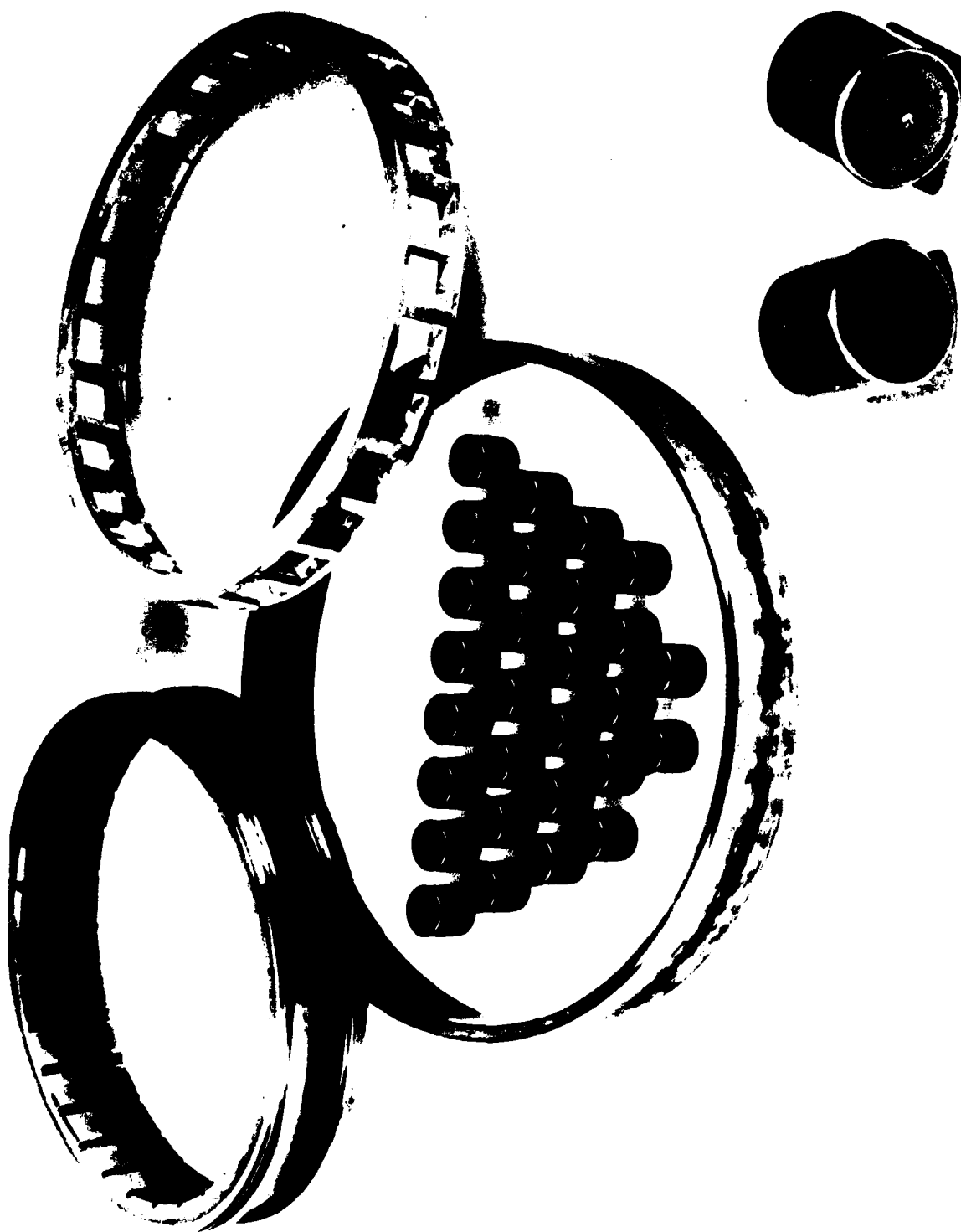
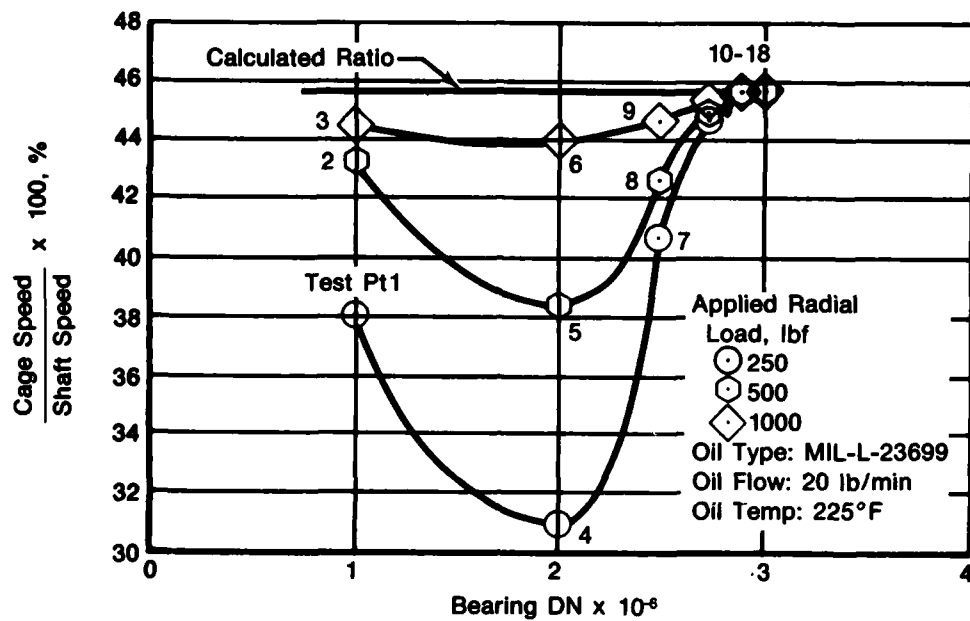
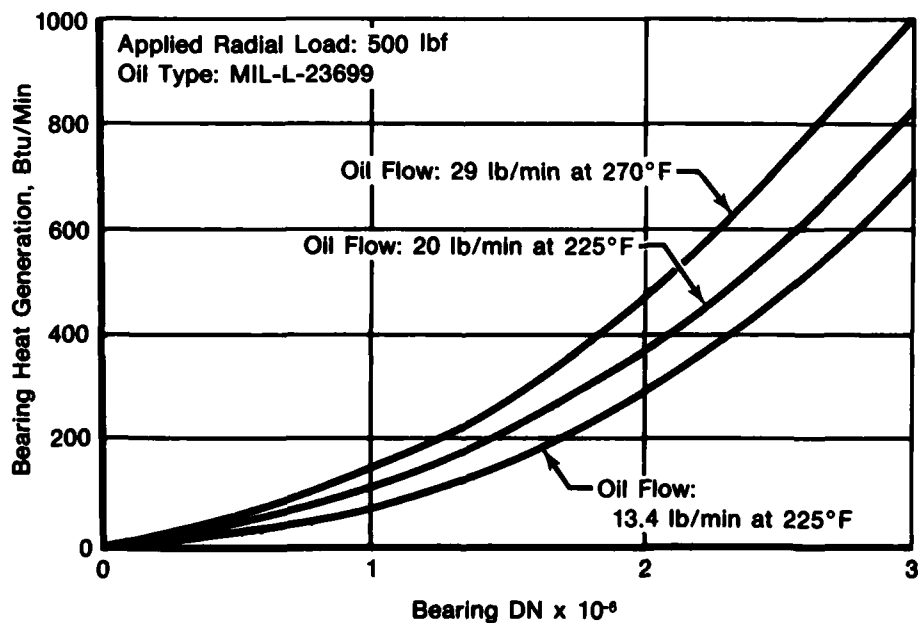


Figure 12. Components of Bearing No. 27 Appear in Good Condition After 10 Hours of Test. Light Concentric Roller End Wear Noted.
FD 100266



FD 184189

Figure 13. Decreased Roller Skid is Observed as Radial Load Is Increased on Bearing No. 27. No Skid Was Noted at Speeds Above 2.9 MDN



FD 184190

Figure 14. Increasing Oil Flow Results in Increased Heat Generation for Bearing No. 27

Experimental Evaluation of Parametric Bearing No. 28

Bearing No. 28 was the third parametric design to be experimentally evaluated. As shown in Figure 4, this design was manufactured with a high inner ring guide flange height and baseline equivalent levels for the remaining three study parameters. The bearing completed the 10-hour program without interruption and with stable performance noted throughout. Roller pass frequency measurements indicated that skid was occurring in the range of 1.0 to 2.75 MDN as had been observed for bearings No. 31 and 27. As seen in Figure 16, roller skid at 2.75 was approximately 0.6% for all applied loads with effectively no skid at 2.9 and 3.0 MDN. Again, the highest skidding occurred at 2.0 MDN, with the maximum amount of skid occurring at the lowest radial load of 250 lbf. Thermal performance of this bearing is shown in Figures 17 and 18 and is similar to that observed for bearings No. 31 and 27. Post-test inspection of the bearing components revealed that all were in good condition as shown in Figure 19 with no significant distress or unusual wear noted. The wear that did occur on the rollers was evidenced by only very light eccentric wear patterns on both end faces. Roller weight measurements confirmed that the wear level was low with an average loss of only 0.0003 grams per roller recorded. It was also determined that the static skew angle change was very low with an average increase of 0.93 minutes per roller observed.

Experimental Evaluation of Parametric Bearing No. 29

The next parametric bearing experimentally evaluated was No. 29. Referring to Figure 4, this bearing design included a low flange height, a greater than normal amount of roller end clearance, and a high level of roller flat off-set. The bearing was installed in the test rig and completed the 10-hour program without interruption. Roller pass frequency measurements indicated that skid was occurring from the onset of testing. As observed for the previously tested bearings, the maximum skid occurred at 2.0 MDN with the greatest amount occurring with the lowest applied radial load. A complete survey of the cage speed relative to the shaft speed was not obtained due to a failure of the roller pass frequency measurement instrumentation during the calibration portion of the test. The thermal performance of bearing No. 29 is shown in Figures 20 and 21, and is similar to that observed for the previously tested bearings. Post-test inspection conducted on bearing No. 29 showed all of the components to be in good condition, Figure 22. No significant distress or unusual wear of the components was observed and examination of the rollers indicated the presence of a combination of light concentric and very light eccentric end wear patterns. Roller and guide flange wear was low as indicated by the low average roller weight loss of only 0.0004 grams and the small skew angle average increase of 5.27 minutes per roller.

Experimental Evaluation of Parametric Bearing No. 30

Bearing No. 30 as shown in Figure 4, included a high inner ring guide flange height, a greater than normal amount of roller end clearance, and a high level of roller flat off-set. Testing progressed through the 10-hour program without incident. Instrumentation measurements indicated that the roller elements were skidding over the speed range of 1.0 to 2.75 MDN. Roller skid at 2.75 MDN varied from approximately 1.0% with a 1000 lbf load to 10.0% with the 250 lb load, see Figure 23. As experienced with the previously tested bearings, the greatest magnitude of skid occurred at 2.0 MDN. Stable operation of the bearing was noted throughout the 3.0 MDN steady state endurance testing with no skidding indicated. The thermal performance, Figures No. 24 and 25, of parametric bearing No. 30 was nearly identical to that observed for the designs tested previously under this program. Post-test inspection revealed all of the test components to be in good condition with only light concentric wear in evidence on the ends of all the rollers, see Figure 26. The wear rate for bearing design No. 30 was extremely low with only 0.0003 grams of average roller weight loss and 1.17 minutes of average skew angle increase per roller determined.

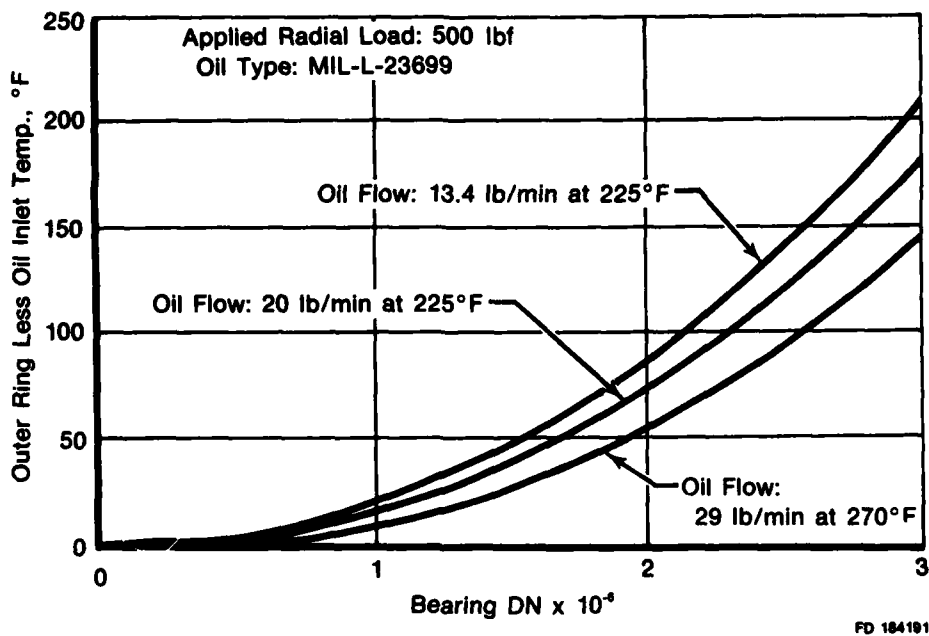


Figure 15. Increasing Oil Flow Results in Reduced Outer Ring-to-Oil Inlet Temperature Differential for Bearing No. 27

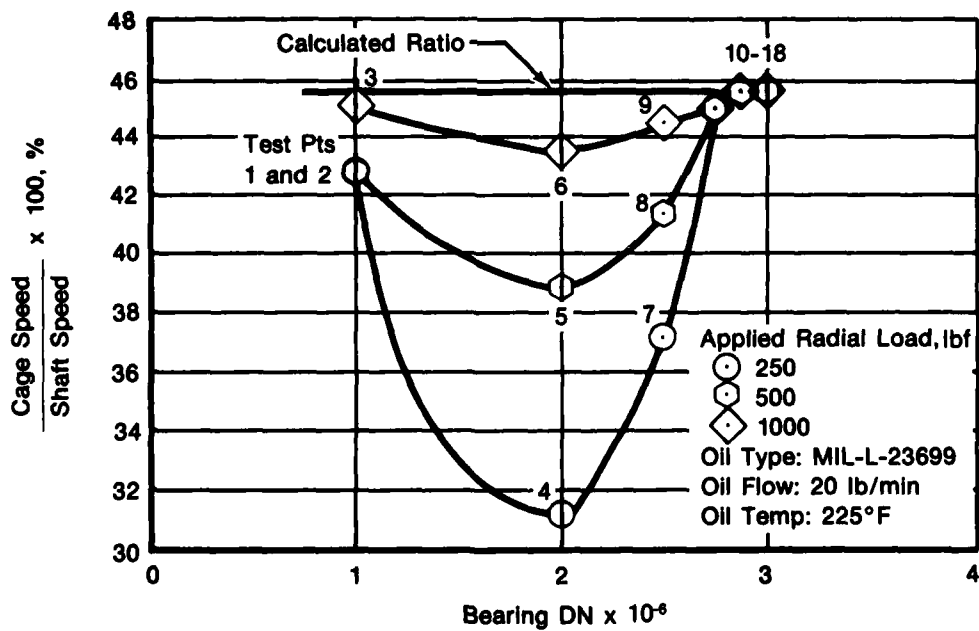
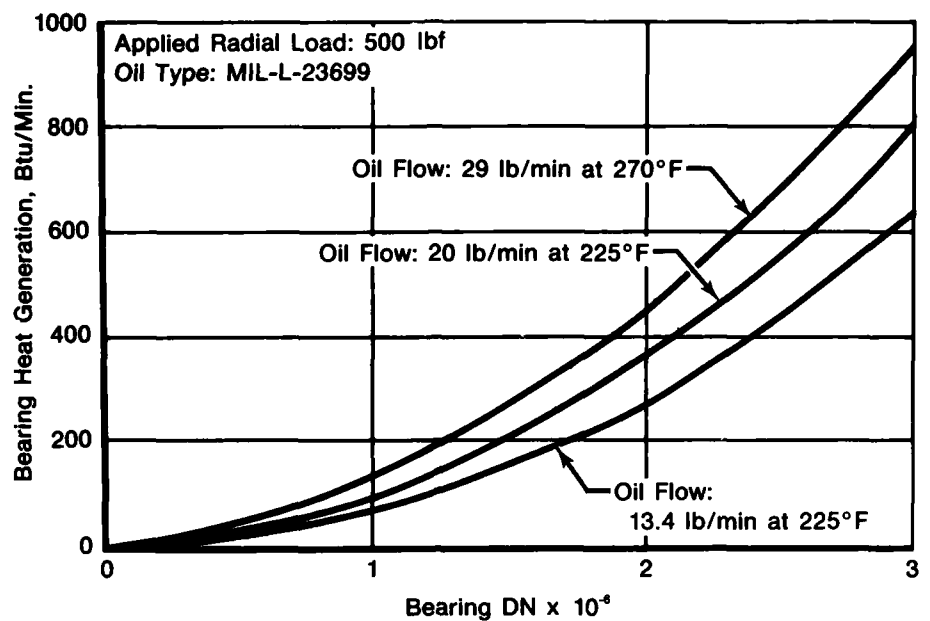
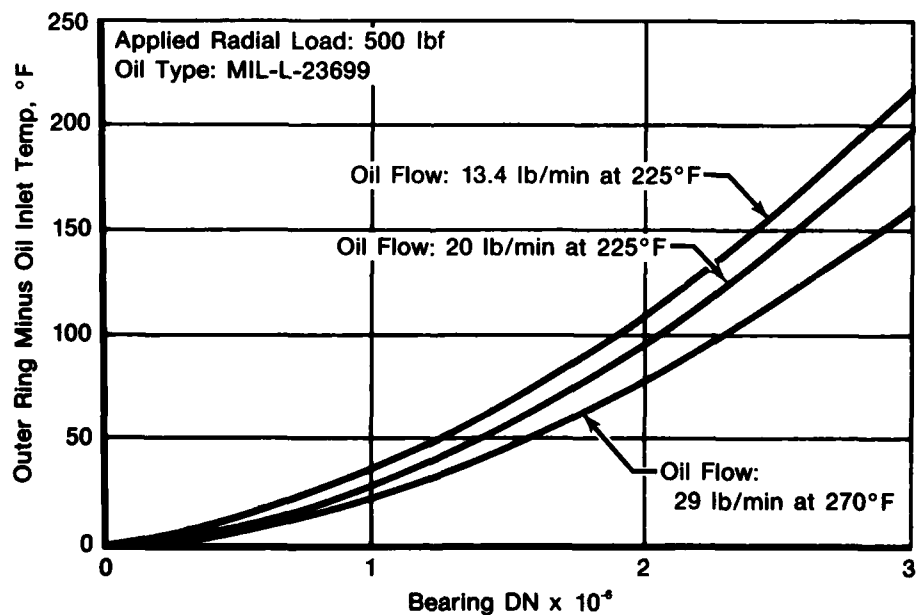


Figure 16. Increasing Applied Load Reduces Roller Skid on Bearing No. 28 With No Skidding Above 2.9 MDN



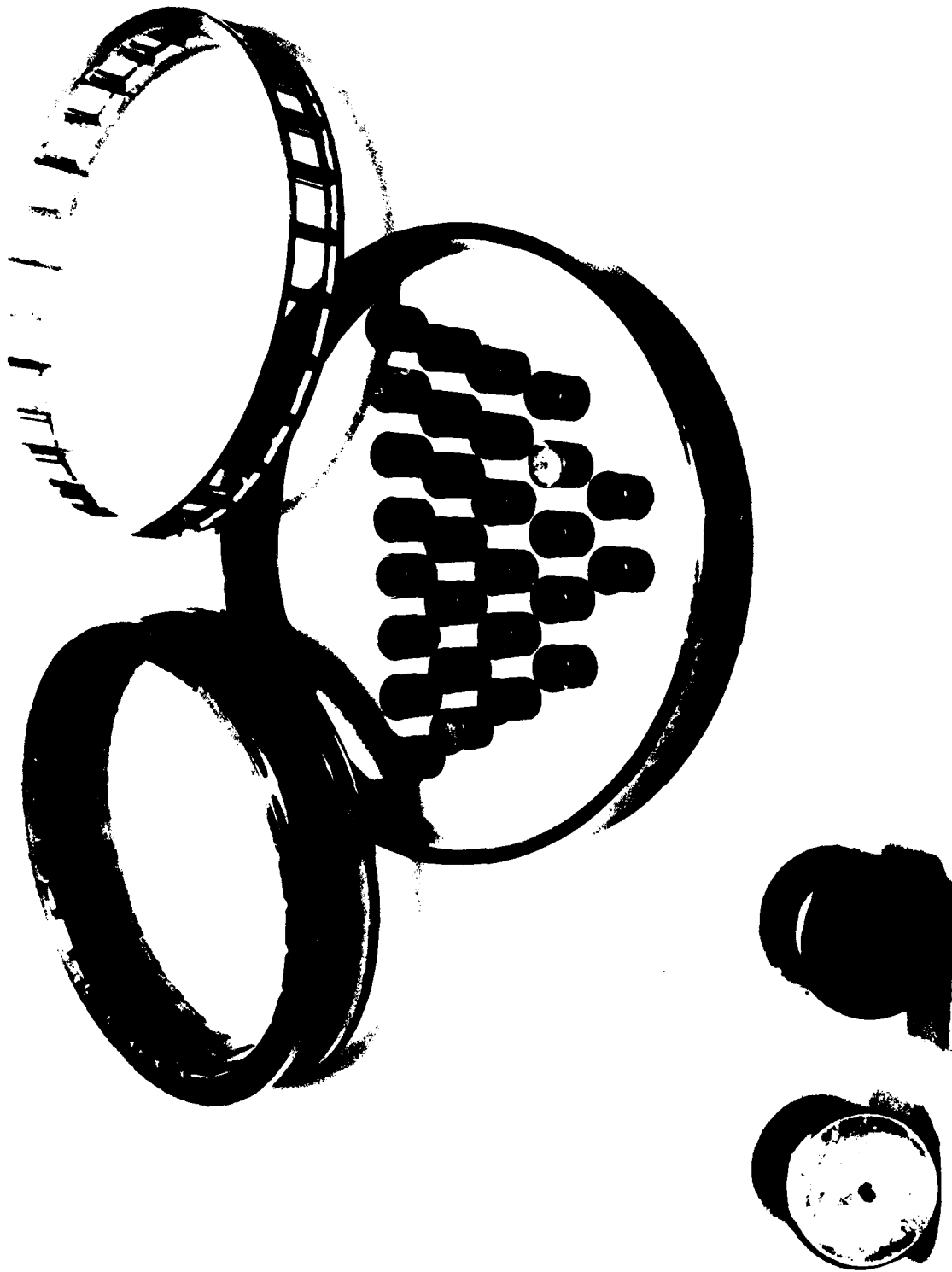
FD 184193

Figure 17. Increasing Oil Flow Results in Increased Heat Generation for Bearing No. 28



FD 184194

Figure 18. Increasing Oil Flow Results in Decreased Outer Ring-to-Oil Inlet Temperature Differential for Bearing No. 28



FD 100258

Figure 19. Components of Bearing No. 28 Appear in Good Condition After 10 Hours of Test. Very Light Eccentric Wear Is Present on Roller Ends

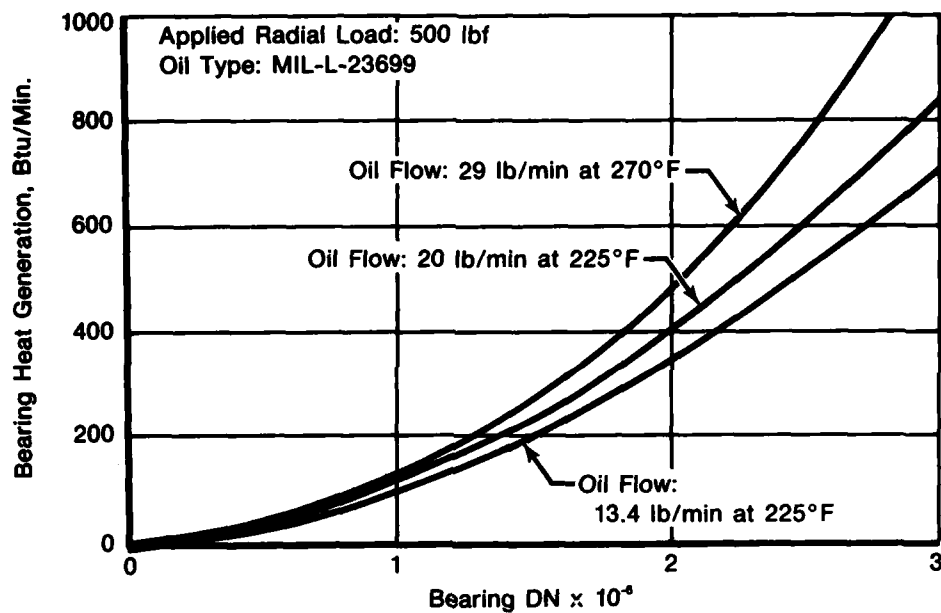


Figure 20. Increasing Oil Flow Results in Increased Heat Generation for Parametric Bearing Design No. 29

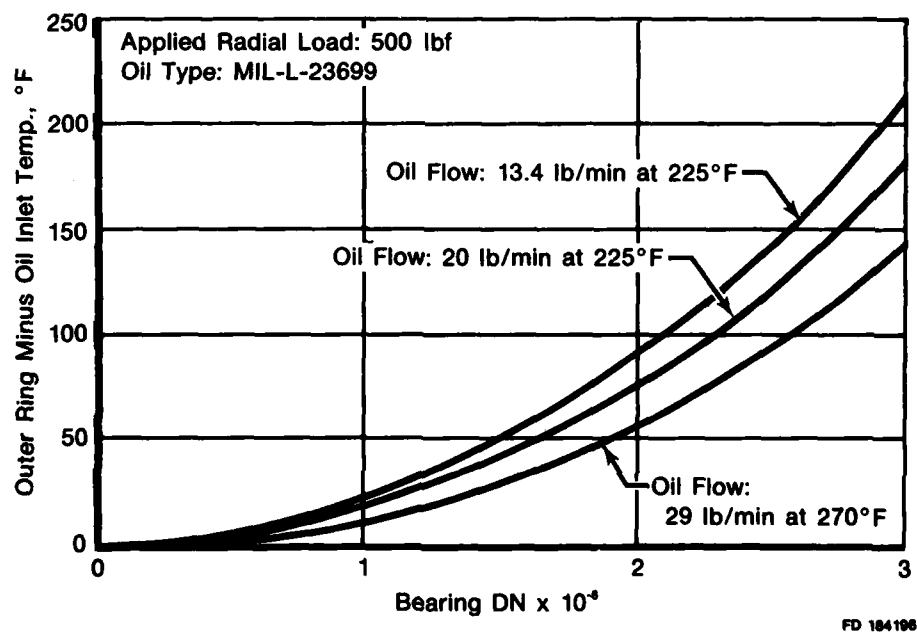


Figure 21. Increasing Oil Flow Results in Reduced Outer Ring-to-Oil Inlet Temperature Differential for Bearing No. 29

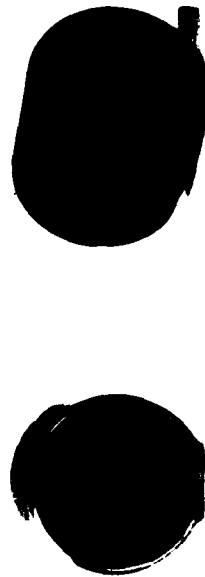
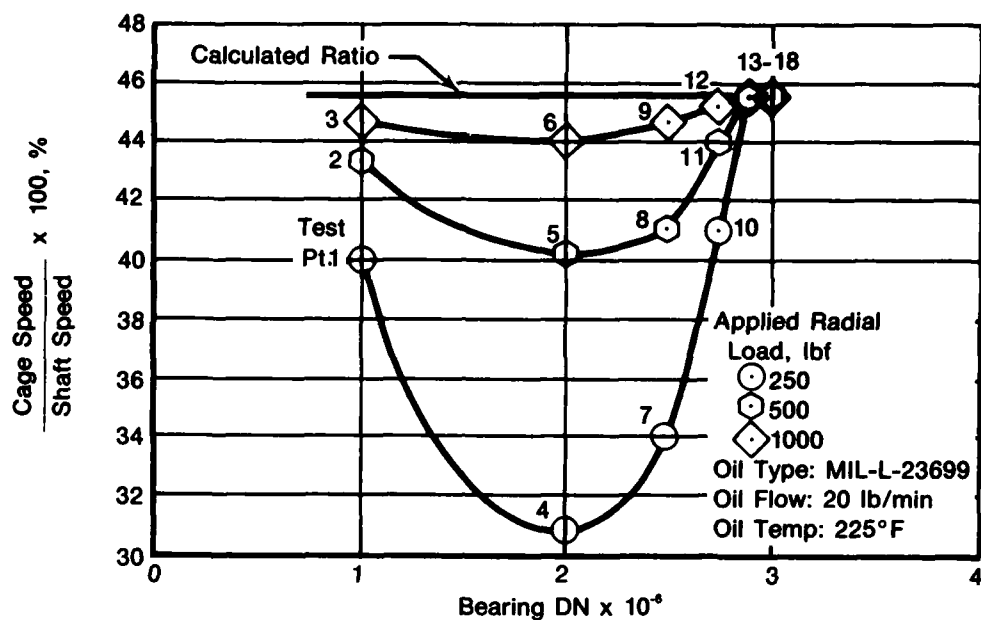


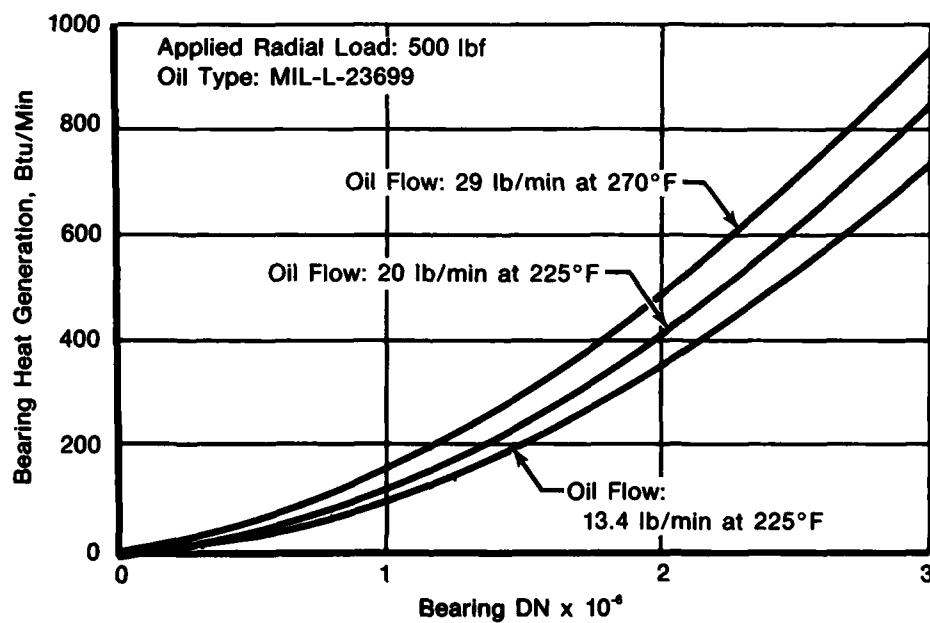
Figure 22. Components of Parametric Bearing Design No. 29 Appear in Good Condition After 10-Hour Test. Light Concentric and Very Light Eccentric Wear are Present on Roller Ends

FD 103250



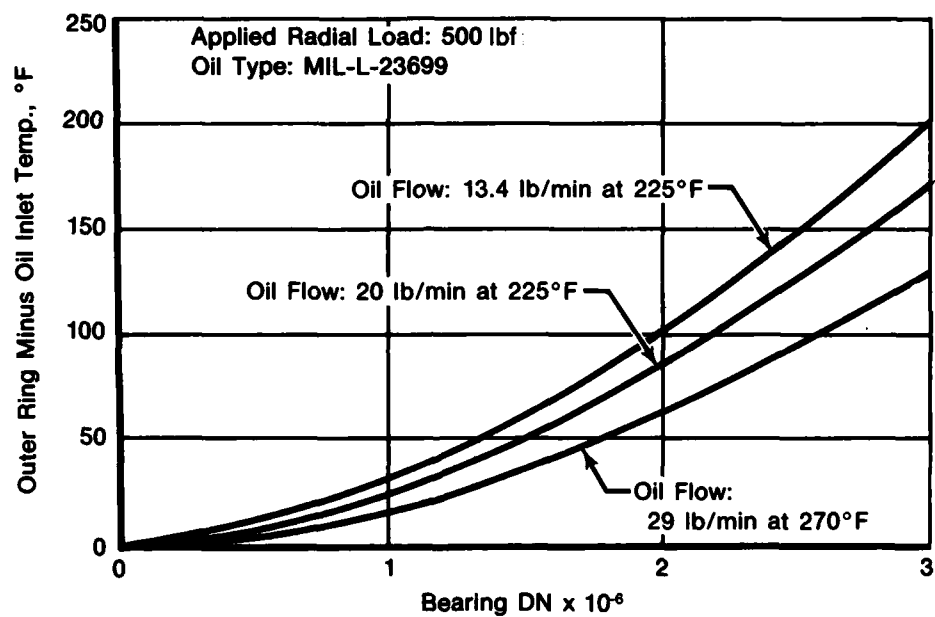
FD 184197

Figure 23. Increasing Applied Load Reduces Roller Skid on Bearing No. 30 With No Skidding Above 2.9 MDN



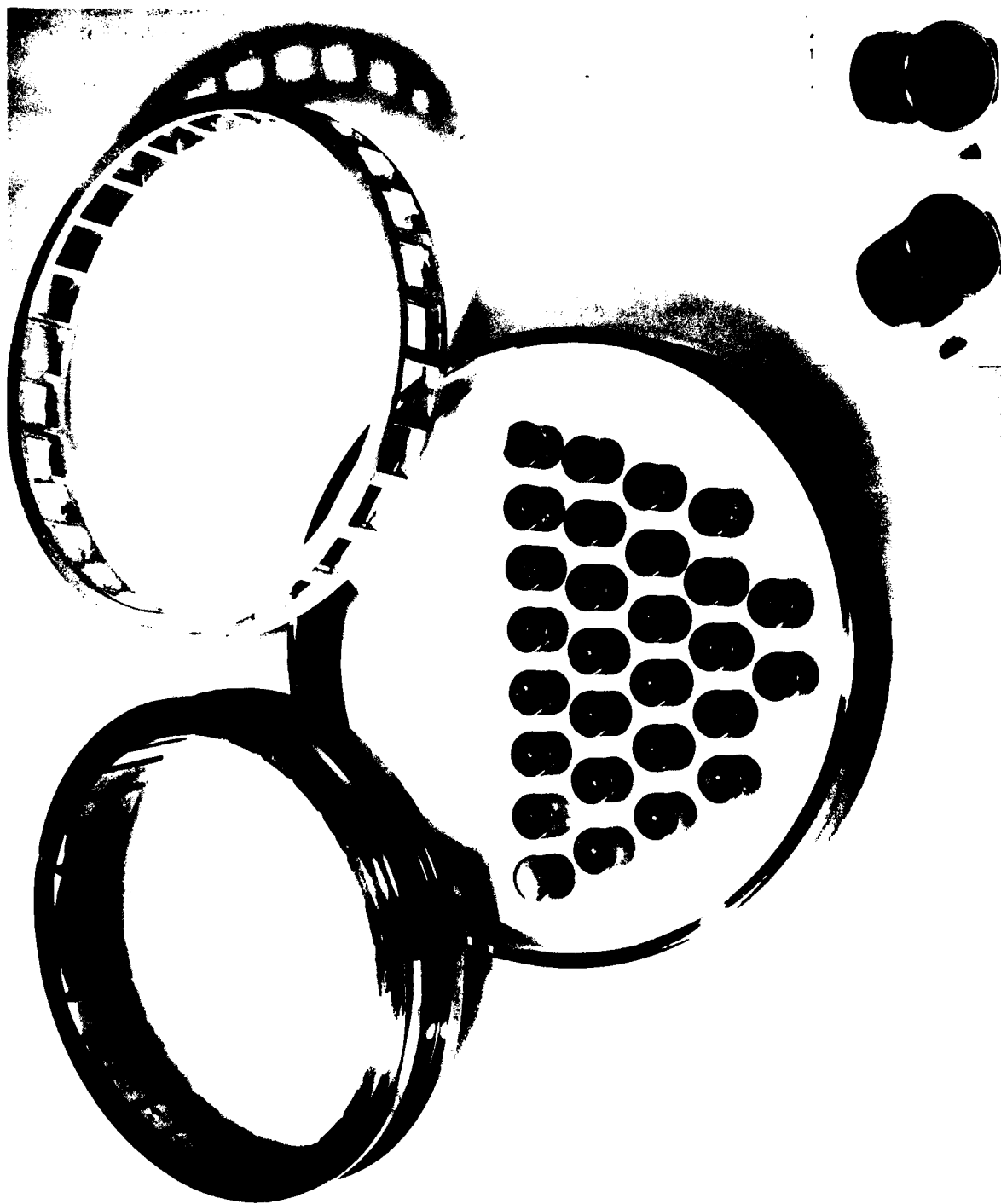
FD 184198

Figure 24. Increasing Oil Flow Results in Increased Heat Generation for Bearing No. 30



FD 184199

Figure 25. Increasing Oil Flow Results in Reduced Outer Ring-to-Oil Inlet Temperature Differential for Bearing No. 30



FD 103240

Figure 26. Components of Parametric Bearing Design No. 30 Show Low Wear and No Distress After 10-Hour Test. Light Concentric Wear Is Present on Both Ends of Rollers

Experimental Evaluation of Parametric Bearing No. 32

The final parametric design to be experimentally evaluated was bearing No. 32 which contained high levels of inner ring guide flange height, roller end clearance, and roller flat off-set. Testing progressed smoothly with the 10-hour run being completed without interruption. Roller skidding was observed over the speed range of 1.0 to 2.75 MDN as was the case with all of the bearings previously evaluated in this program. Referring to Figure 27, roller element skid at 2.75 MDN varied from approximately 1.0% under a radial load of 1000 lbf to 4.0% with a 250 lbf load. As observed in the previous tests the maximum degree of skidding occurred at 2.0 MDN coincident with the lowest applied load. Throughout the evaluation stable operation was noted and the thermal performance as shown in Figures 28 and 29 was observed to be similar to that previously measured for the other five bearings. Post-test observations proved all of the components to be in good condition, Figure 30, with no distress or unusual wear of the components noted. Although both concentric and eccentric wear patterns were observed on the roller ends, the degree of wear was light. The average roller weight change was determined to be 0.0022 grams while the average roller skew angle increased 11.41 minutes.

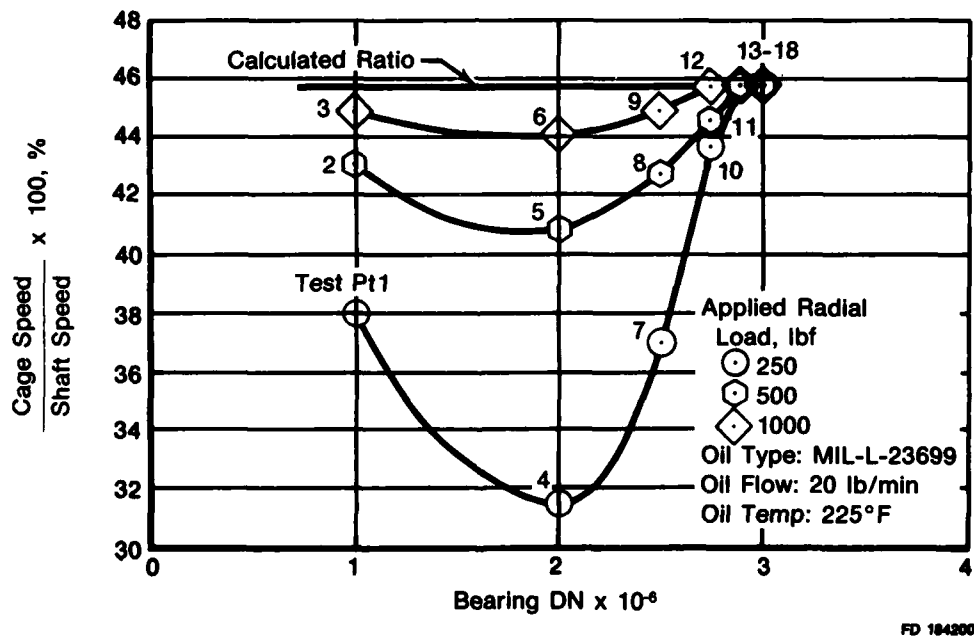


Figure 27. Increasing Applied Radial Load Reduces Roller Skid on Bearing No. 32 With No Skidding Above 2.9 MDN

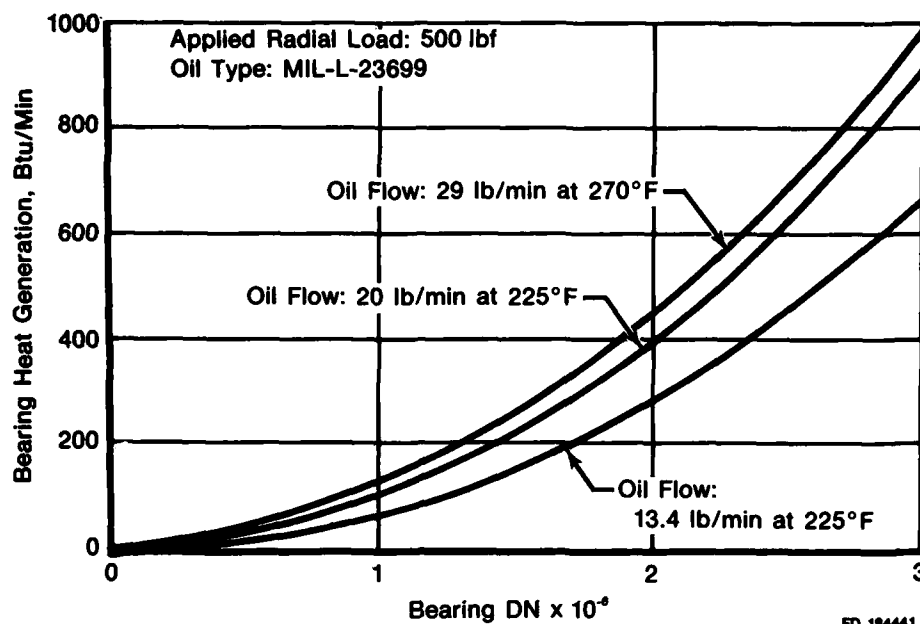


Figure 28. Increasing Oil Flow Results in Increased Heat Generation for Bearing No. 32

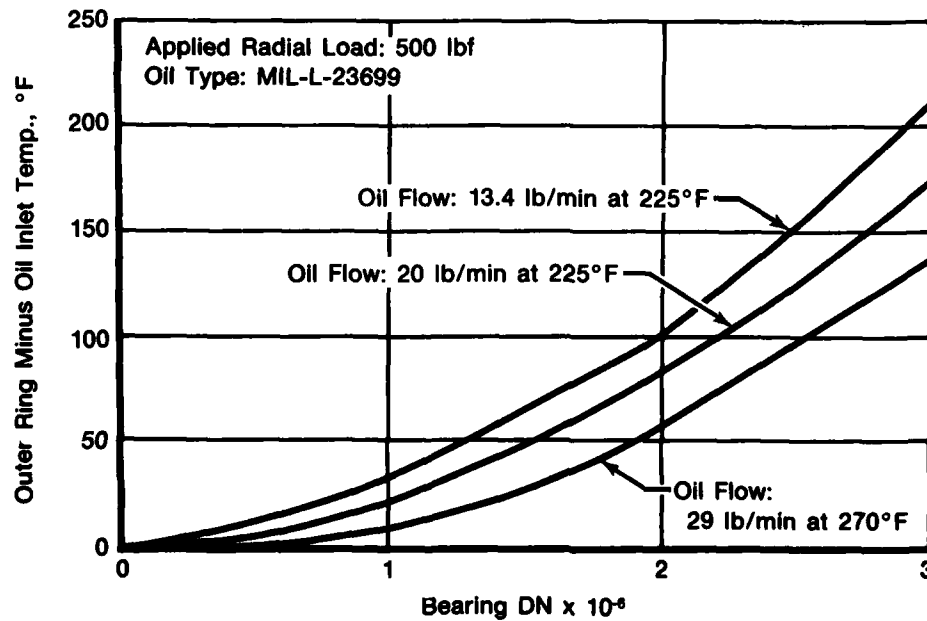
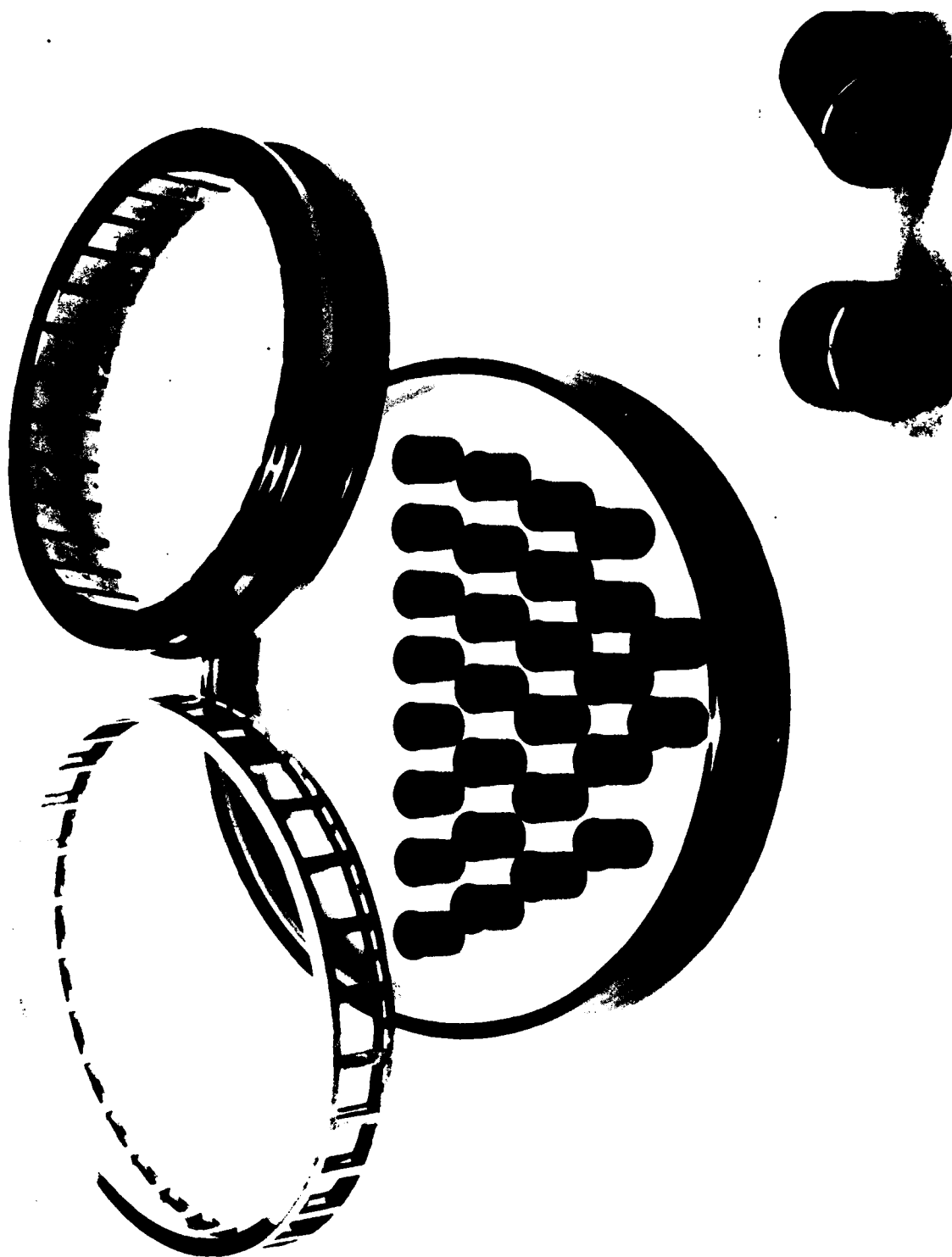


Figure 29. Increasing Oil Flow Results in Reduced Outer Ring-to-Oil Inlet Temperature Differential for Bearing No. 32



FD 183261

Figure 30. Components of Parametric Bearing Design No. 32 Appear in Good Condition After 10-Hour Test. Light Concentric and Eccentric Wear Observed on Roller Ends

SECTION III BEARING TEST ANALYSIS AND CORRELATION — PHASE II

STATISTICAL ANALYSIS OF THE EXPERIMENTAL WEAR RESULTS

The statistical analysis of the test data was completed in order to determine the effects of the four independent bearing parameters on roller end wear. Roller end wear was determined by measuring roller weight loss and roller skew angle change. Regression and correlation analysis of the wear results summarized in Table 9 were utilized to rank the bearing parameters affecting each response. The specific independent parameters evaluated are identified as follows:

- VAR 1 — Roller End Circular Runout
- VAR 2 — Roller Flat Centrality
- VAR 3 — Roller End Clearance
- VAR 4 — Inner Ring Guide Flange Height

The above factors were considered the controlled variables of the test program and were varied as shown in Figure 4. At least two levels for each variable were preselected and represent values encountered in the manufacturing or design process. The six bearing designs containing the four controlled variables were defined in order to allow the linear contribution of each variable on bearing life to be examined statistically.

In addition, initial roller static skew angle was analyzed as another independent variable which was varied but not controlled in the experimental test program. Initial roller static skew angle is a function of several variables including roller end clearance and inner ring guide flange height. In separate high speed experimental tests at P&WA on larger diameter cylindrical roller bearings, a relationship was observed between initial roller skew angle and roller end wear.

The main parameters affecting roller bearing life in this program are considered to be average roller weight loss and static skew angle change per hour of testing. Therefore, these two variables, considered as dependent in the statistical analysis of the test data, are expressed as follows:

Y_1 , Average Weight Change

Y_2 , Average Skew Angle Change

Multiple regression equations were developed from the data by the method of least squares. Each equation yields the mean value of one of the dependent variables. The equations therefore yield expected performance of a roller bearing under stated conditions. Prior to the development of the actual regression equations, a mathematical model was in each instance formulated relating the independent variables to the dependent variable. The general form of the mathematical model is a multivariate polynomial in which the coefficients appear linearly. The terms in each model are candidates for inclusion in the fitted regression equation.

TABLE 9. ROLLER WEIGHT AND SKEW ANGLE WEAR DATA OBTAINED FROM THE EXPERIMENTAL EVALUATION OF THE GROUP-AF4 BEARINGS

Bearing No.	Parameters				Roller Wear Results			Magnitude and Type of Wear
	Roller End Cir. Runout to Roller OD inch	Roller Flat Centrality, inch	Roller End Clearance, inch	Roller End Flange Height, % Roller dia	Avg Roller Weight Loss, grams	Avg Roller Skew Angle increase		
Baseline	0.00012	0.010	0.001	25				
27	0.0001	0.050	0.001	20	0.0022	0°9.86'	Moderate/Concentric and Slight Eccentric	
28	0.0002	0.010	0.001	30	0.0003	0°0.93'	Light/Eccentric	
29	0.0002	0.050	0.002	20	0.0004	0°5.27'	Light/Concentric and Slight Eccentric	
30	0.0001	0.050	0.002	30	0.0003	0°1.17'	Light/Concentric	
31	0.0001	0.010	0.005	20	0.0061	0°32.43'	Heavy/Concentric	
32	0.0002	0.050	0.005	30	0.0022	0°11.41'	Moderate/Slight Eccentric	

The general model takes the form:

$$Y = b_0X_0 + b_1X_1 \dots + b_nX_n + e = \hat{Y} + e$$

where Y is the observed value of a particular dependent variable, either Y₁ or Y₂, \hat{Y} is the corresponding value of the dependent variable computed from the expression involving the X's and the b's, where the X's are the values of the independent variables, the b's are the coefficients to be estimated from the experimental data, and e represents the differences between observed and estimated values of the dependent variable due to residual variation or experimental error in the observations.

The data set appropriate for each model was computer analyzed to determine the values of the regression coefficients and other relevant statistics. The regression models determined for each dependent variable, Y₁ and Y₂, are shown in Tables 10 and 11 respectively. The information presented includes:

- Variable name
- COEFFICIENTS: calculated values of regression coefficients, b_i
- CONF BAND: Confidence Band calculated as a function of t Table value for a given level of confidence, b_i, and S_{b_i}
- STD ERR: Standard error coefficient, S_{b_i}
- T-VALUE: calculated t value, b_i/S_{b_i}

TABLE 10. MULTIVARIATE LINEAR REGRESSION
FOR AVERAGE ROLLER WEIGHT CHANGE,
Y₁

	Coefficient	Conf Band	Std Err	T-Value
Constant	0.87361			
VAR 1	-0.11534D-02	+/- 0.519192E-02	0.408813E-03	-2.82
VAR 2	-2.3679	+/- 16.1583	1.27231	-1.86
VAR 4	-0.14919D-01	+/- 0.654237E-01	0.515147E-02	-2.90
VAR 5	0.99578	+/- 1.95702	0.154096	6.46

Percent Variability Explained = 98.659; SEE = 0.58109E-01

Correlation Between Y OBS and Y CAL = 0.99327; N = 6; T = 12.70

Dependent Variable is Y.

$$\text{VAR 5} = -0.2139 \text{ VAR 3} + 0.04612 (\text{VAR 3})^2,$$

where VAR 5 is the curvilinear effect of roller end clearance VAR 3, on roller weight loss, see Figure 33.

TABLE 11. MULTIVARIATE LINEAR REGRESSION FOR
AVERAGE ROLLER SKEW ANGLE CHANGE,
Y₂

	<i>Coefficient</i>	<i>Conf Band</i>	<i>Std Err</i>	<i>T-Value</i>
Constant =	43.642			
VAR 1 =	-0.43469D-01	+/- 0.297565	0.234303E-01	-1.86
VAR 2 =	-130.34	+/- 913.578	71.9353	-1.81
VAR 4 =	-0.94241	+/- 3.74677	0.295021	-3.23
VAR 6 =	0.98993	+/- 2.13881	0.168410	5.88

Percent Variability Explained = 98.389; SEE = 3.3278

Correlation Between Y OBS and Y CAL = 0.99191; N = 6; T = 12.70

Dependent Variable is Y₂.

$$\text{VAR 6} = -6.773 \text{ VAR 3} + 1.741 (\text{VAR 3})^2,$$

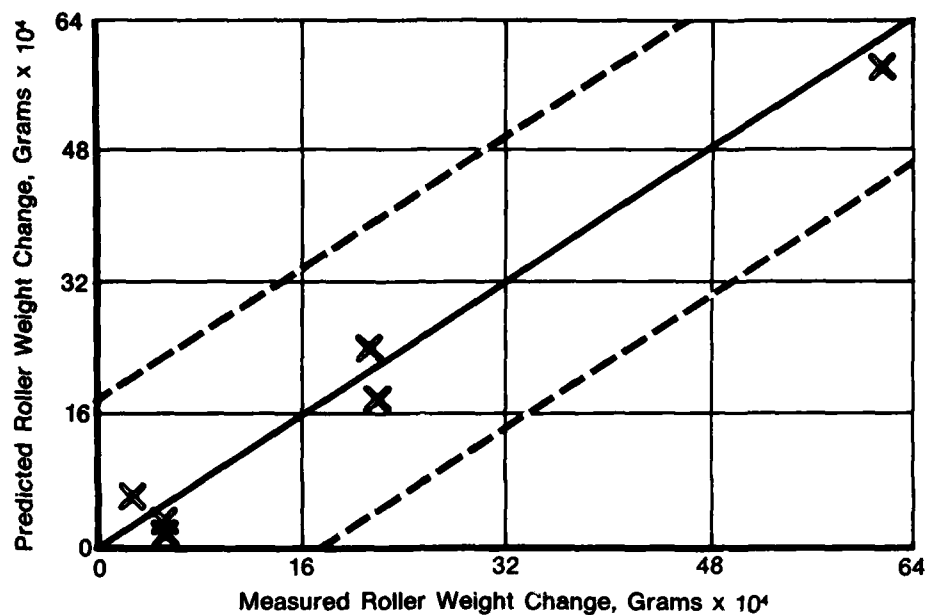
where VAR 6 is the curvilinear effect of roller end clearance, VAR 3,
on roller skew angle change, see Figure 37.

The T-value parameter permits the evaluation of each term in the response regression equation with the largest absolute value indicating that which is the strongest or most important bearing variable in the group. The sign indicates the direction of the effect, i.e. a positive sign signifies that an increase in the magnitude of the controlled variable results in an increase in roller weight loss and/or skew angle change, whereas a negative sign means that an increase of the magnitude of the controlled variable results in a decrease in roller weight loss and/or skew angle change.

Other statistics of interest are presented in Tables 10 and 11 and are the following:

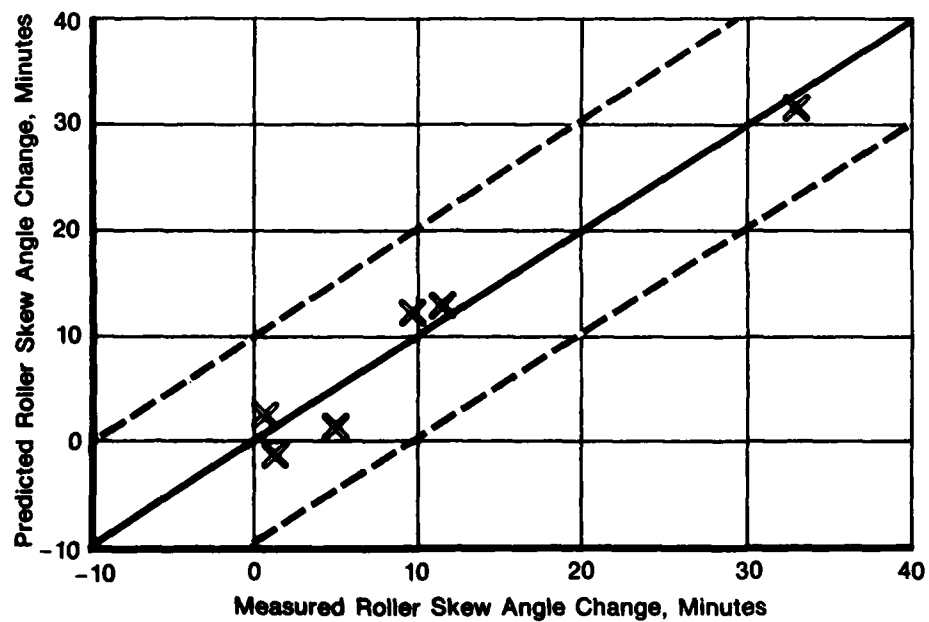
- PERCENT VARIABILITY EXPLAINED, R², which is the square of the multiple correlation coefficient R, is a measure of the proportion of variation in the dependent variable accounted for by the regression equation.
- The SEE or Standard Error of Estimate, is the magnitude of the error in predicting the output parameter.
- R, the correlation between Y OBS and Y CAL, is an index indicating the degree of association between Y OBS and Y CAL, where a value of 1.0 indicates a perfect fit, i.e. no experimental error, and a value of 0 indicates no association, i.e. large experimental error.
- N is the sample size.
- T is the Student Table T-value which is to be exceeded by the calculated T-VALUE in order to define a statistically important factor at 95% confidence.

A graphical analysis of the regression models are presented in Figure 31 for Y₁, roller weight change and in Figure 32 for Y₂, roller skew angle change. In these analyses, the ordinate represents the calculated wear characteristic and the abscissa is the measured wear characteristic. These figures display the excellent correlation obtained between the predicted and measured wear values where a perfect or ideal correlation would yield all data points on the 45° line.



FD 184443

Figure 31. Excellent Correlation Is Shown Between Measured and Predicted Roller Weight Loss



FD 184444

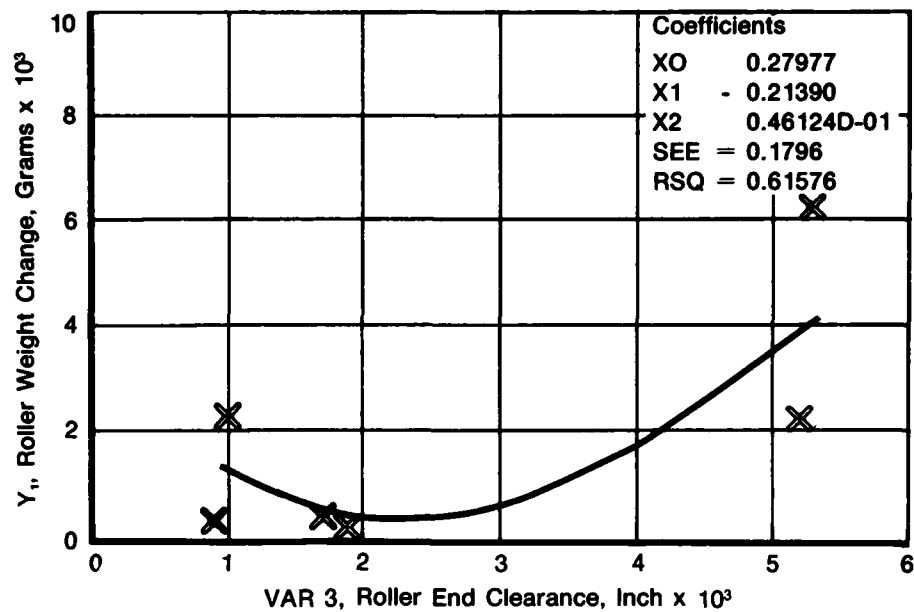
Figure 32. Excellent Correlation Is Shown Between Measured and Predicted Roller Skew Angle Change

The statistical analysis of Y_1 , roller weight change, indicates that this dependent variable is significantly affected by roller end clearance, VAR 3. A curvilinear effect is shown and can be seen in Figure 33 which predicts minimum wear near the intermediate level of parametric variation. Secondary effects are shown in Figure 34 for inner ring guide flange height, VAR 4, and in Figure 35 for roller end circular runout, VAR 1. These secondary effects as indicated by the slope are both negative. The fourth study variable, roller flat centrality, VAR 2, does not have a significant effect on roller weight change. The statistical analysis of the dependent variable Y_2 , roller skew angle change, indicates similar effects for the program variation of the independent parameters as those observed for the other dependent parameter, roller weight change. This is due to the strong correlation between these two dependent parameters as shown in Figure 36. This correlation allows the prediction of one of the dependent variables given a value for the other.

The regression analysis, Table 11, indicates that roller end clearance, VAR 3, significantly affects static skew angle change. The curvilinear effect, Figure 37, is similar to that shown for roller weight change. A secondary effect for inner ring guide flange height, VAR 4, is also shown and as indicated in Figure 38 this effect is negative. No significant effects, however, are identified for either roller end circular runout, VAR 1, or roller flat centrality, VAR 2.

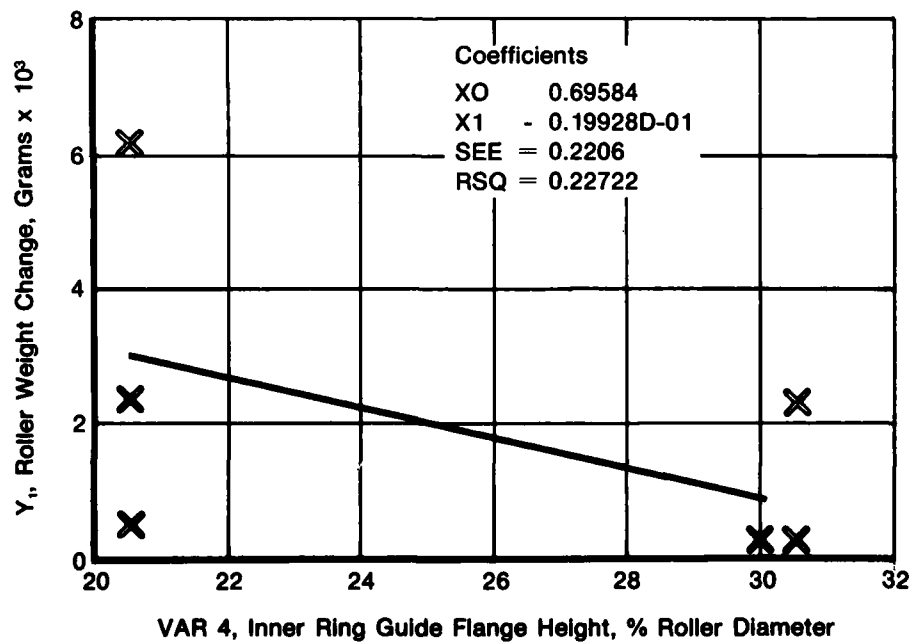
The uncontrolled parameter, initial roller static skew angle, VAR 7, was also analyzed using the pretest bearing measurements from Table 5. As indicated by the regression models shown in Figures 39 and 40, initial skew angle has a positive effect on the wear parameters. Therefore, for reduced roller and guide flange wear, reduced initial skew angle is desired. Figure 41 shows initial skew angle as a function of roller end clearance for the two different levels of guide flange height investigated. Figure 42 shows initial skew angle as a function of guide flange height for the three levels of roller end clearance. The results indicate that the initial roller skew angle is affected more by end clearance than shoulder height for ranges of these variables that would be practical for a high speed bearing design.

A summary of the statistically analyzed roller weight loss and skew angle change results are presented in Table 12. Shown here are the combinations of the parameter variation levels which yield minimum wear characteristics and are therefore recommended for high speed roller bearing design. No significant end wear effects could be determined for either roller end circular runout, VAR 1, or roller flat centrality, VAR 2, for the levels tested. It would seem that high levels of either of these parameters would have a destabilizing effect on roller motion and thus possibly lead to roller end wear. A possible explanation for this apparent contradiction may be that the range of magnitudes tested for these variables was not large enough to allow identification of their significance. In this light then, it is not necessary to alter the baseline roller flat centrality specification of 0.010 in. In addition, end circular runouts up to 0.000180 FIR are allowable. Roller end clearance should be specified at or near the 0.002 level, and the inner ring guide flange height should be designed to the high level of 30% of the roller diameter. It should be noted that the manufactured value of roller axial clearance was not changed significantly due to installation into the test rig. These conclusions are based on the experimental results obtained under this program which were generated exclusively on 124 mm size bearings. In addition, the results are based on the levels of parameter variation selected for study.



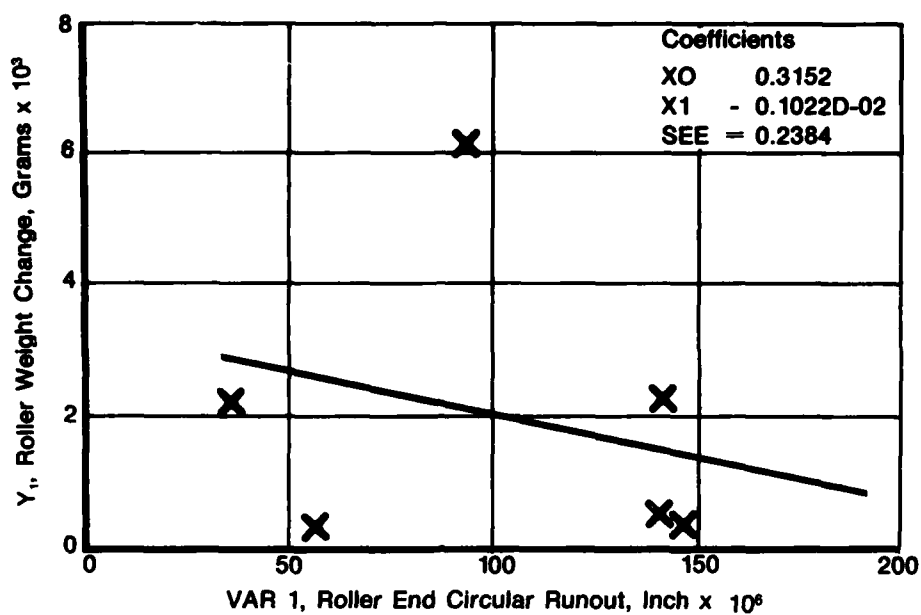
FD 184445

Figure 33. Curvilinear Effect of Roller End Clearance on Roller Weight Loss



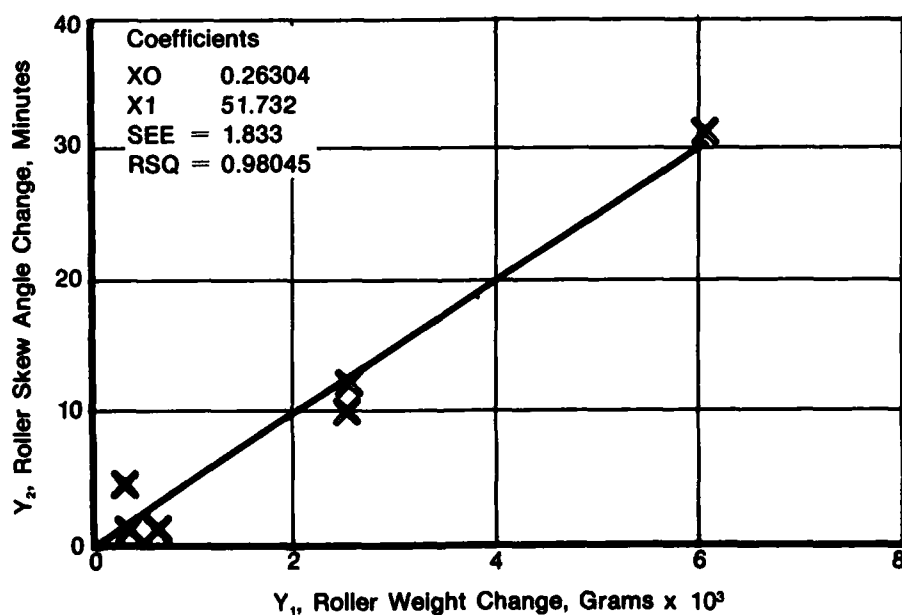
FD 184446

Figure 34. Inner Ring Guide Flange Height Shows Slight Negative Effect on Roller Weight Loss



FD 184447

Figure 35. Roller End Circular Runout Shows Slight Negative Effect on Roller Weight Loss



FD 184448

Figure 36. Good Correlation Is Shown Between Roller Weight Loss and Skew Angle Change

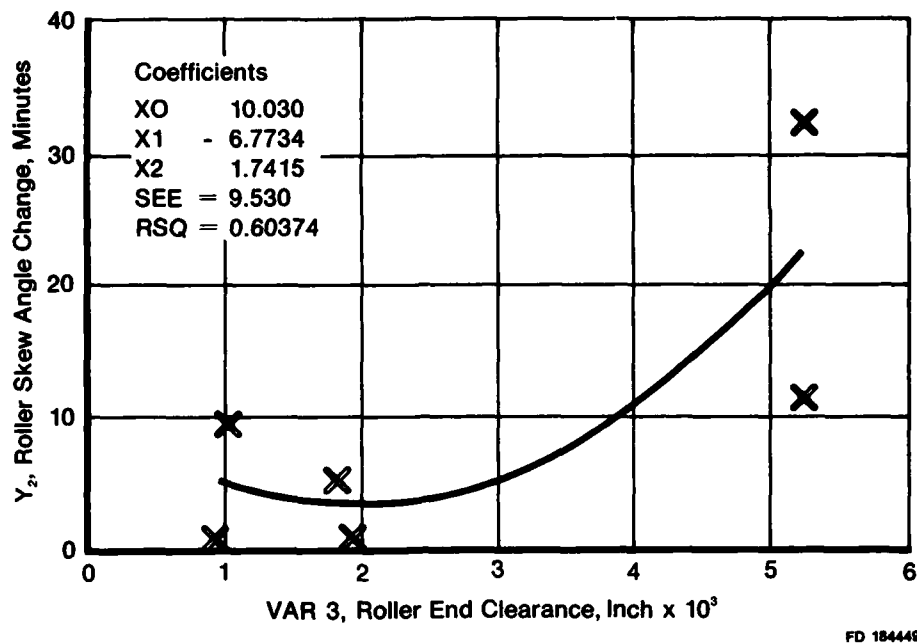


Figure 37. Curvilinear Effect of Roller End Clearance on Roller Skew Angle Change

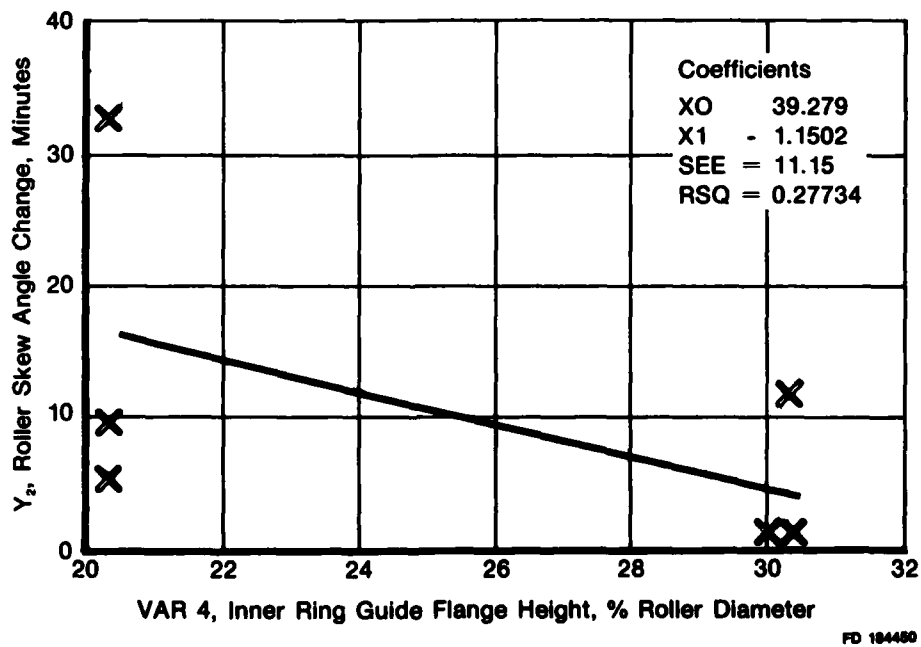


Figure 38. Inner Ring Guide Flange Height Shows Slight Negative Effect on Roller Skew Angle Change

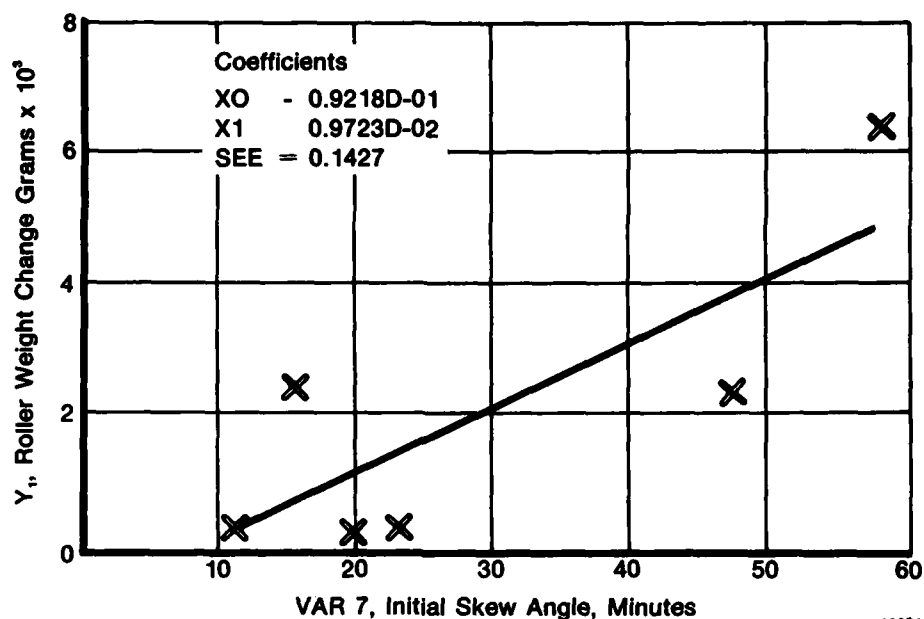


Figure 39. Initial Roller Skew Angle Shows Positive Effect on Roller Weight Change

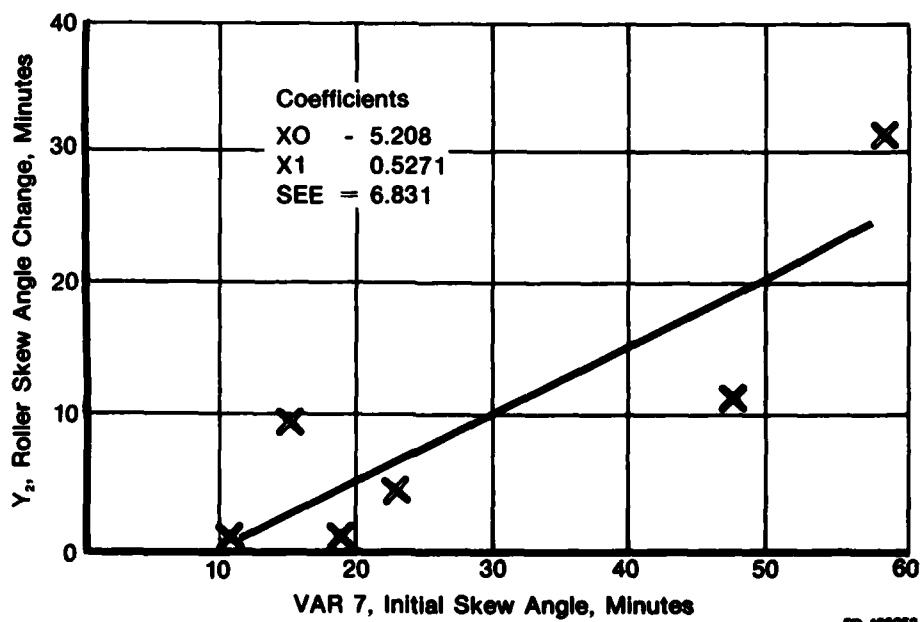


Figure 40. Initial Roller Skew Angle Shows Positive Effect on Roller Skew Angle Change

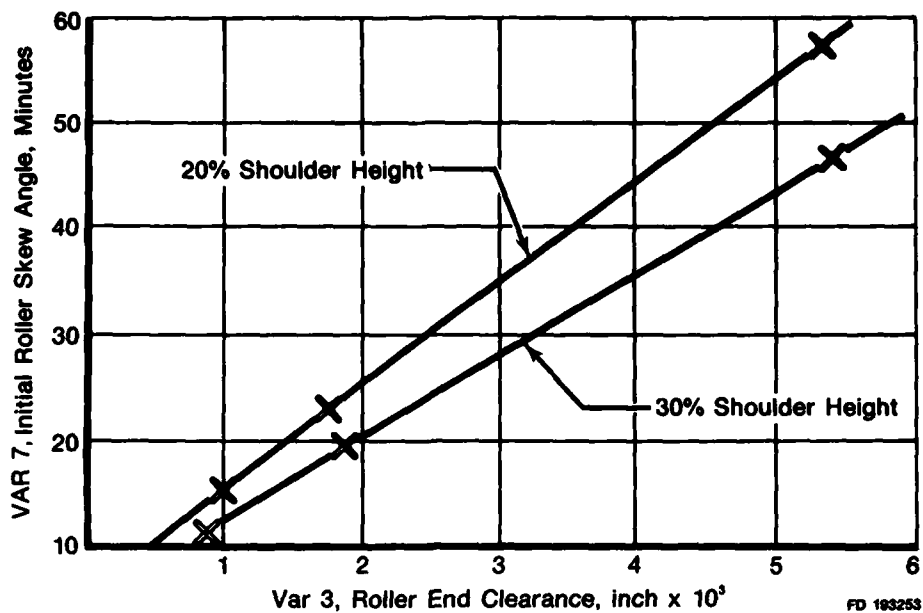


Figure 41. Roller End Clearance Shows a Significant Positive Effect on Initial Roller Static Skew Angle

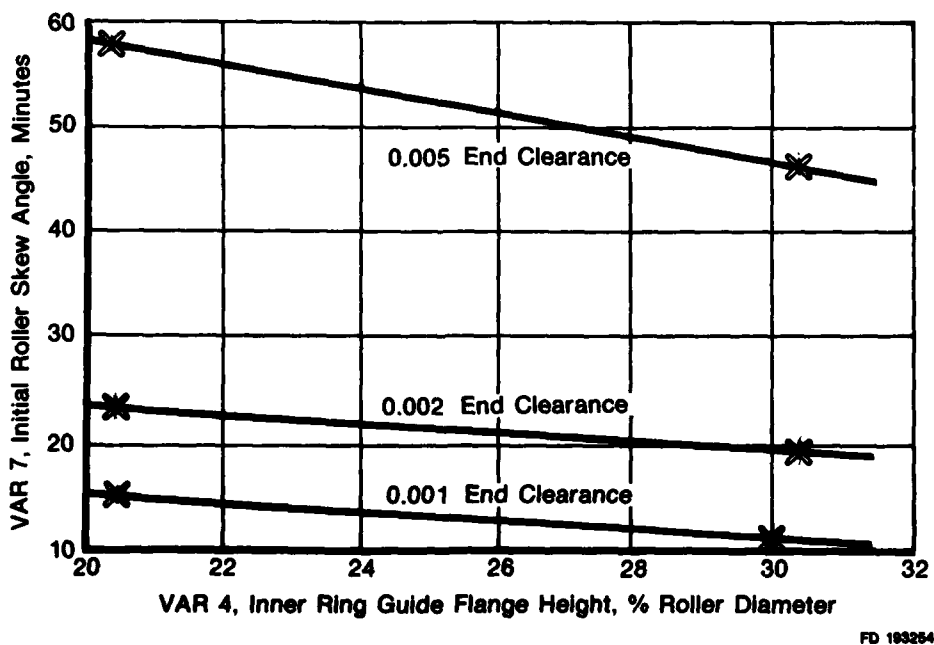


Figure 42. Inner Ring Guide Flange Height Shows Only a Moderate Negative Effect on Roller Initial Skew Angle

TABLE 12. PARAMETRIC ROLLER BEARING EXPERIMENTAL WEAR RESULTS

Variable	Levels Tested				Min Wear Predicted	Avg Roller Weight Average	Avg Roller Skew & Change
	Baseline	Low	Med	High			
Roller end circular runout, inch $\times 10^{-6}$	120	50	—	180	180	1	—
Roller flat centrality, inch $\times 10^{-3}$	10	10	—	50	—	—	—
Roller end clearance, inch $\times 10^{-3}$	1	1	2	5	2	1*	1*
Inner ring guide flange height, % roller dia.	25	20	—	30	30	1	1

— No effect on output

! Trend with output is curvilinear, select intermediate or medium level

! Trend with output is negative, select higher level

* Indicates a significant roller bearing variable

CORRELATION OF ANALYTICAL MODEL

The analytical model and the associated computer program, TRIBO-I, which are being developed under the NAPC contract, References 1 and 2, will provide a means of predicting roller bearing dynamic performance. In addition, the computer program will provide predictions of bearing heat generation, ring temperatures, cage speed, and roller mass loss due to wear.

The roller wear model will be correlated with data obtained from the model check testing which was conducted under the NAPC program. The correlation of the cage speed prediction model will be based on test data from both the NAPC contract and this Group-AF4 program. The results of the correlation efforts in both of these areas will be presented in the NAPC contract final report.

The following section deals with the correlation of the thermal model which predicts bearing heat generation and inner and outer ring temperatures.

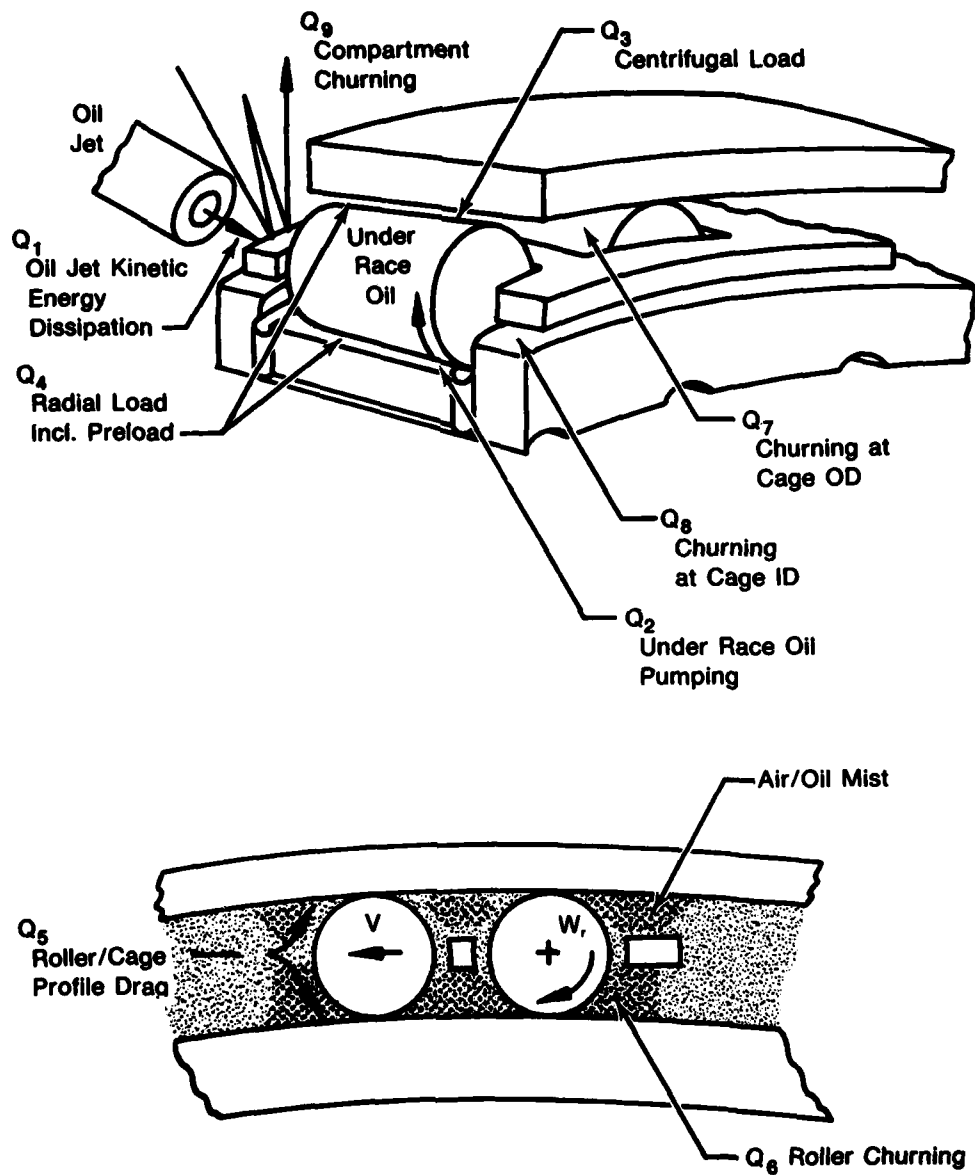
Bearing Heat Generation Correlation

The bearing heat generation analytical model is based on the identification of nine heat generation sources within the operating bearing. The nine sources are shown in the sketches provided in Figure 43. A detailed description of the analytical model will be given in the NAPC contract final report. The results of the correlation of the model with heat generation experimental data from the Group-AF4 testing are given in Figure 44. These curves show the oil heat rejection prediction on the Y-axis versus the experimentally determined heat rejection on the X-axis. The symbols represent three different oil flow rates of 13, 20 and 29 lb/min. A 500 lbf radial load was maintained at each of the DN levels tested. The analytical model predicts total bearing heat generation. The heat rejected to the oil has been found to be approximately 70% of the total bearing heat generation. In general, experimental heat rejection to the oil is within 10% of the predicted values.

Bearing Ring Temperature Correlation

The bearing ring temperature analytical model is a semi-empirical prediction system based on a correlation of cooling effectiveness parameters. A detailed description of the model will be presented in the NAPC contract final report. Results obtained using the model are shown in Figure 45. The curves show the ring temperature prediction on the Y-axis versus the experimentally determined ring temperature on the X-axis. The symbols represent the same operating conditions as for the heat generation curves.

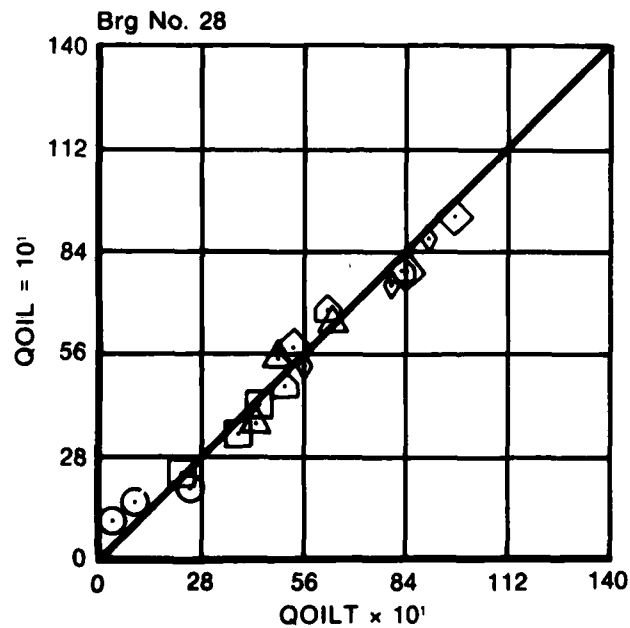
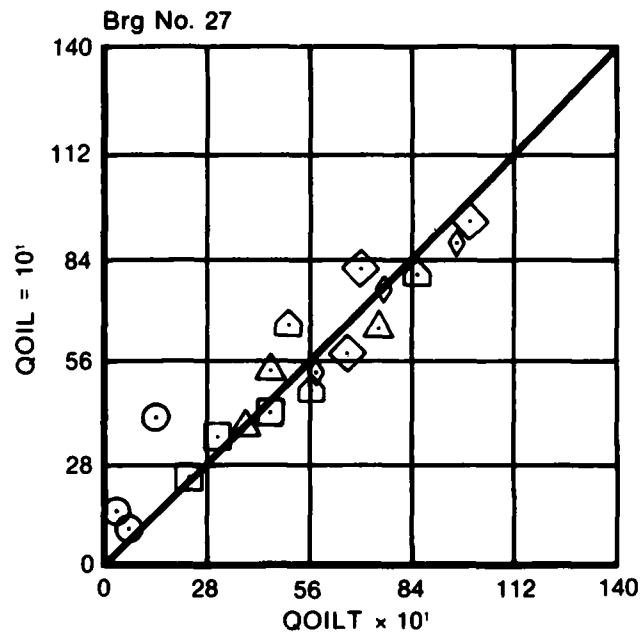
Predicted outer ring temperature is denoted by TOR, and is shown for all six experimental bearings. Since inner ring temperatures were obtained only for bearing No. 31, and significantly more data of this kind were obtained during NAPC contract testing, the correlation for inner ring temperature was based primarily on data from that contract. Figure 45 also illustrates the level of correlation obtained for inner ring temperatures for bearing No. 31. For all test points, the ring temperature prediction is within 10%, improving at the higher DN levels where it approaches 5% of the experimental values.



FD 193255

Figure 43. Bearing Heat Generation Model Identifies Nine Heat Sources Including Drag and Churning Effects Due to Translation and Rotation Through an Air/Oil Environment

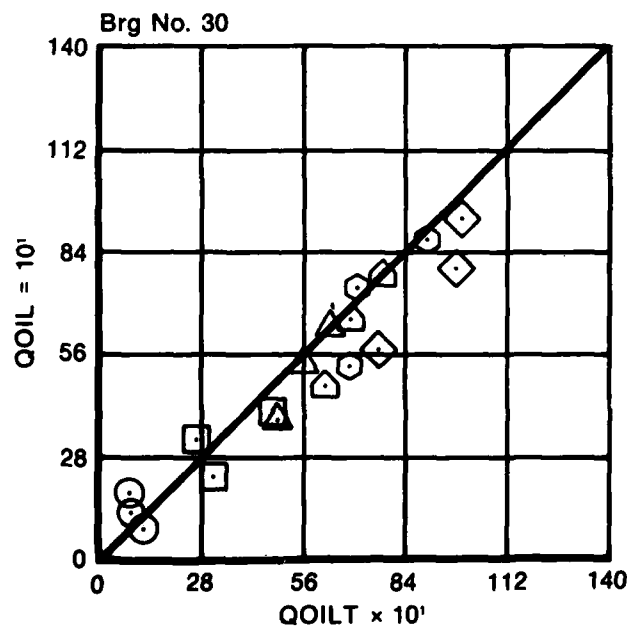
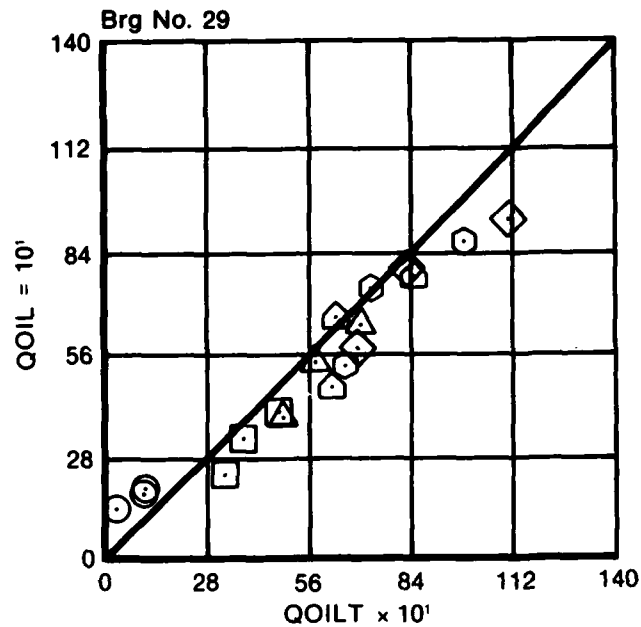
- — 8,045 rpm (1.00 MDN)
- — 16,090 rpm (2.00 MDN)
- △ — 20,113 rpm (2.50 MDN)
- ⬢ — 22,124 rpm (2.75 MDN)
- ⊙ — 23,330 rpm (2.90 MDN)
- ◇ — 24,135 rpm (3.00 MDN)



FD 195112

Figure 44. *The TRIBO-I Thermal Model Provides Good Correlation With Experimental Heat Generation Results (1 of 3)*

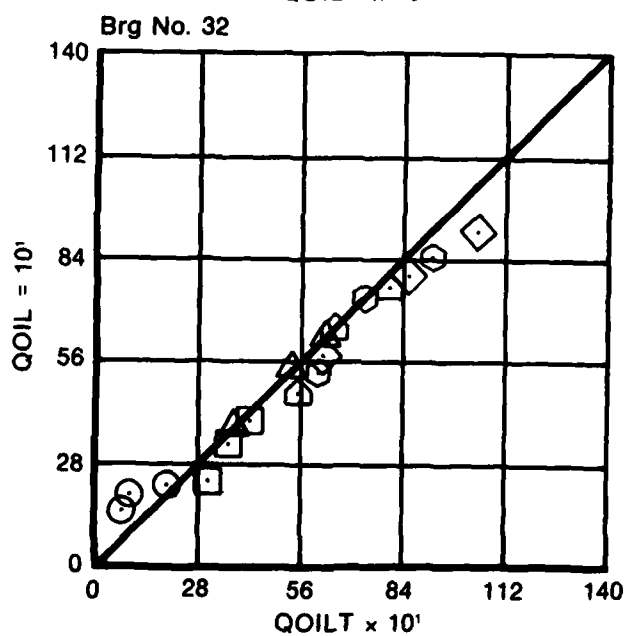
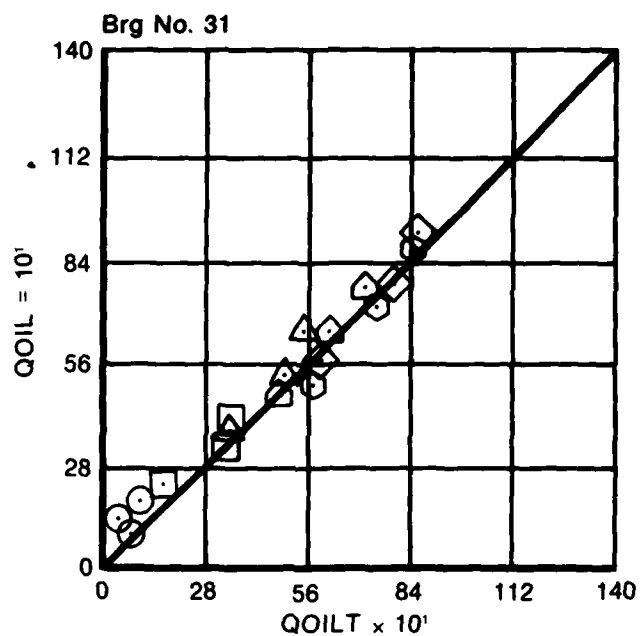
- — 8,045 rpm (1.00 MDN)
- — 16,090 rpm (2.00 MDN)
- △ — 20,113 rpm (2.50 MDN)
- ◻ — 22,124 rpm (2.75 MDN)
- ⊙ — 23,330 rpm (2.90 MDN)
- ◇ — 24,135 rpm (3.00 MDN)



FD 198113

Figure 44. The TRIBO-I Thermal Model Provides Good Correlation With Experimental Heat Generation Results (2 of 3)

- — 8,045 rpm (1.00 MDN)
- — 16,090 rpm (2.00 MDN)
- △ — 20,113 rpm (2.50 MDN)
- ⬢ — 22,124 rpm (2.75 MDN)
- ⊙ — 23,330 rpm (2.90 MDN)
- ◇ — 24,135 rpm (3.00 MDN)



FD 195114

Figure 44. The TRIBO-I Thermal Model Provides Good Correlation With Experimental Heat Generation Results (3 of 3)

- — 8,045 rpm (1.00 MDN)
- — 16,090 rpm (2.00 MDN)
- △ — 20,113 rpm (2.50 MDN)
- ◇ — 22,124 rpm (2.75 MDN)
- — 23,330 rpm (2.90 MDN)
- ◇ — 24,135 rpm (3.00 MDN)

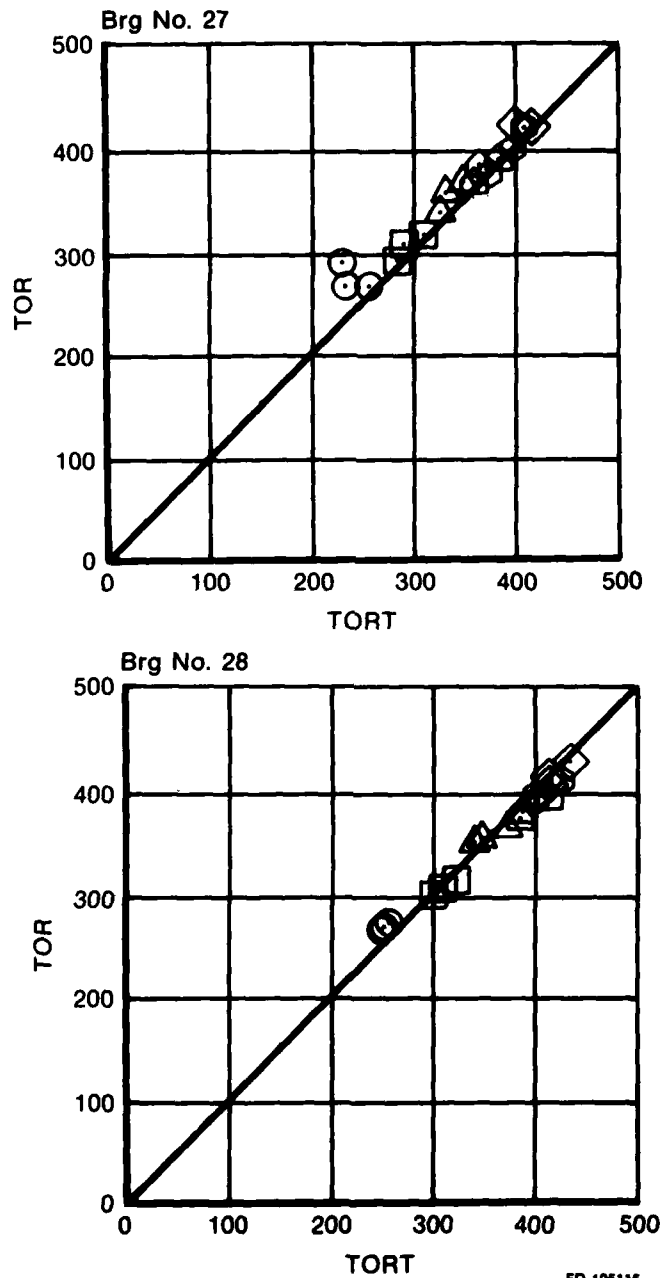
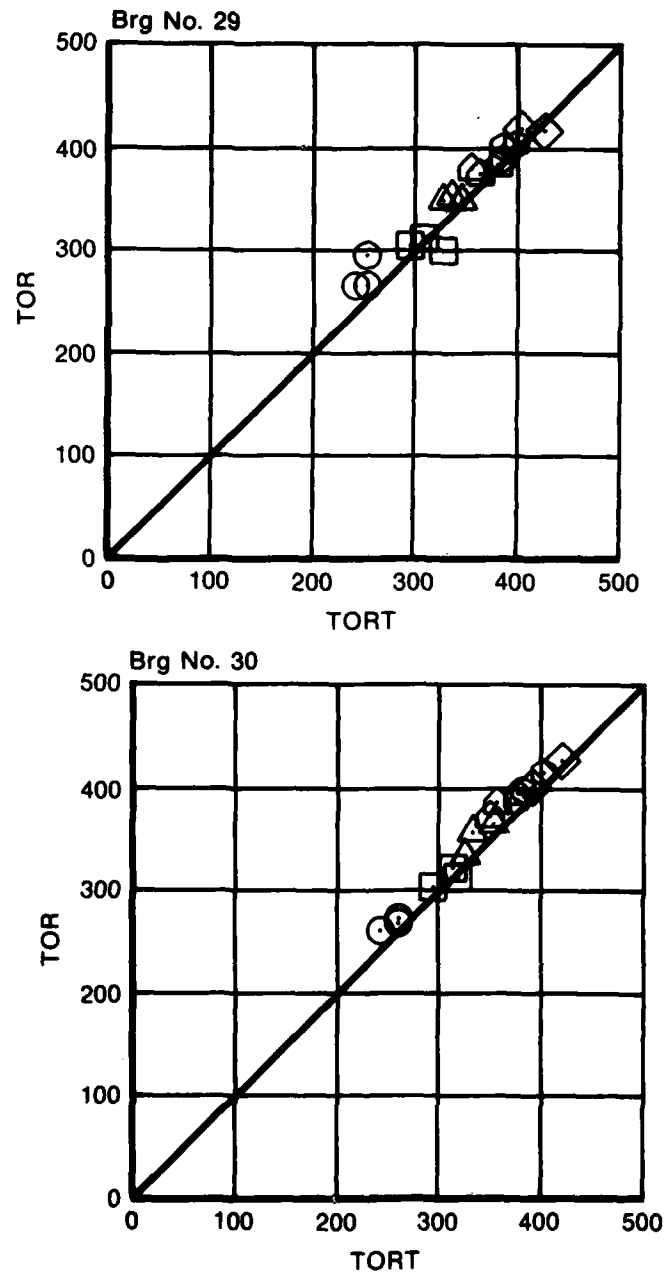


Figure 45. *The TRIBO-I Thermal Model Allows Prediction of Both Inner and Outer Ring Temperatures to Within 10% of Experimental Results (1 of 4)*

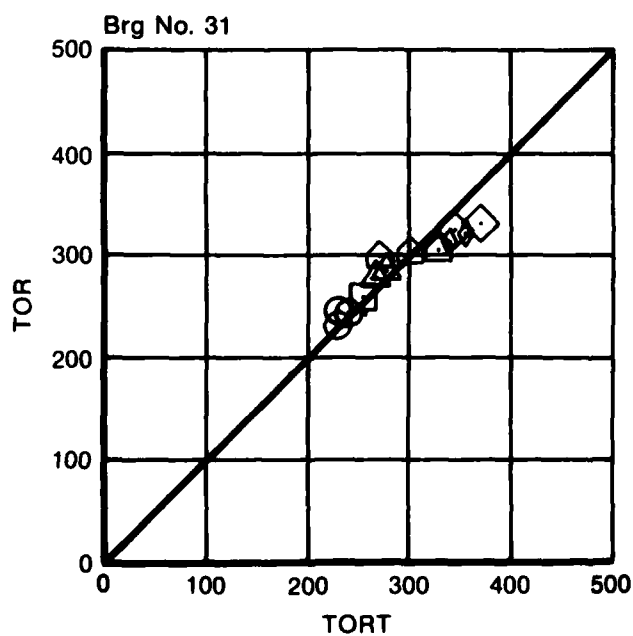
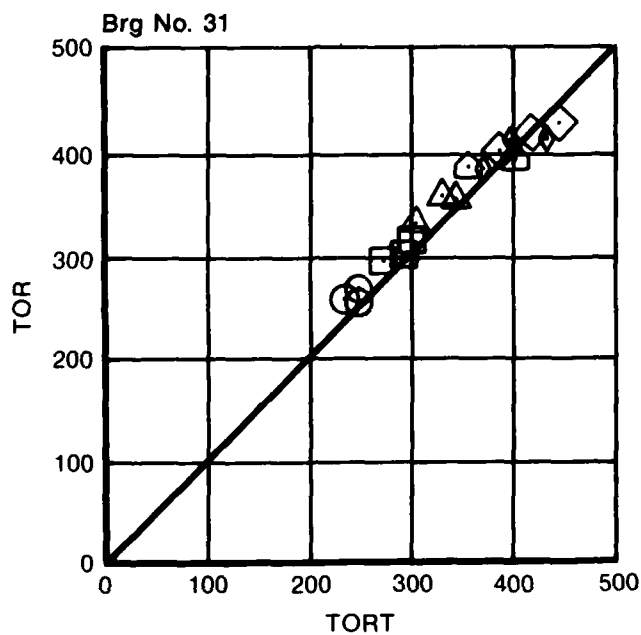
- — 8,045 rpm (1.00 MDN)
- — 16,090 rpm (2.00 MDN)
- △ — 20,113 rpm (2.50 MDN)
- ◇ — 22,124 rpm (2.75 MDN)
- — 23,330 rpm (2.90 MDN)
- ◇ — 24,135 rpm (3.00 MDN)



FD 195117

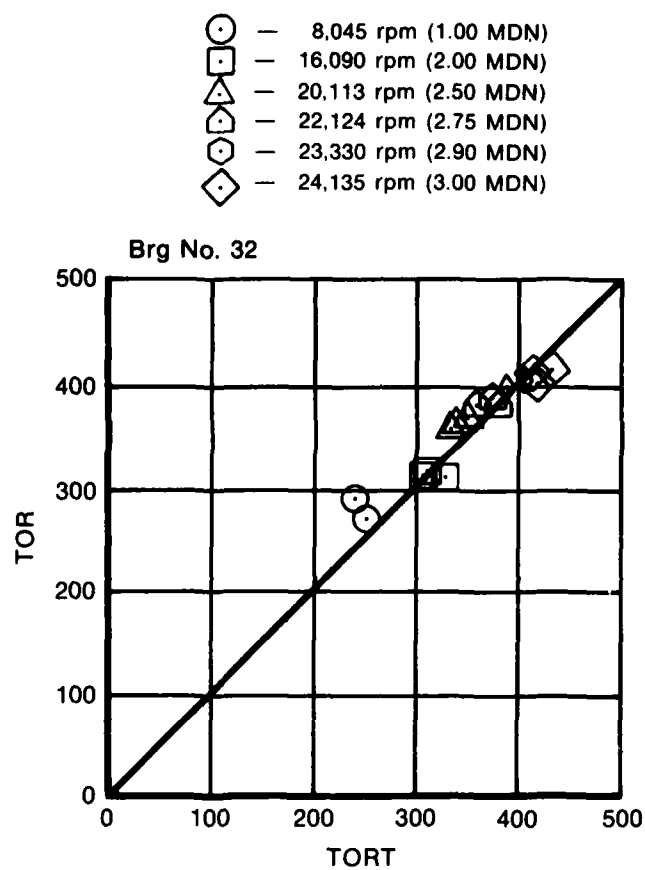
Figure 45. *The TRIBO-I Thermal Model Allows Prediction of Both Inner and Outer Ring Temperatures to Within 10% of Experimental Results (2 of 4)*

- — 8,045 rpm (1.00 MDN)
- — 16,090 rpm (2.00 MDN)
- △ — 20,113 rpm (2.50 MDN)
- ◻ — 22,124 rpm (2.75 MDN)
- ◐ — 23,330 rpm (2.90 MDN)
- ◑ — 24,135 rpm (3.00 MDN)



FD 195116

Figure 45. *The TRIBO-I Thermal Model Allows Prediction of Both Inner and Outer Ring Temperatures to Within 10% of Experimental Results (3 of 4)*



FD 185118

Figure 45. *The TRIBO-I Thermal Model Allows Prediction of Both Inner and Outer Ring Temperatures to Within 10% of Experimental Results (4 of 4)*

SECTION IV CONCLUSIONS AND RECOMMENDATIONS

CONCLUSIONS

Conclusions that can be drawn based on the results accumulated during the experimental evaluation of the 124 mm parametric roller bearings are as follows:

- Of the four parameters studied, roller end clearance was shown to have the most significant effect on roller end and guide flange wear. A curvilinear effect was observed with minimum wear occurring near the intermediate level of end clearance.
- Only moderate effects on wear were observed for both roller end circular runout and inner ring guide flange height for the levels evaluated. Increasing either parameter resulted in reduced wear.
- Increasing roller flat centrality or offset to the level evaluated has no effect on roller end wear.
- Although a wide range of roller and guide flange wear was experienced for the parametric bearings tested, similar thermal characteristics were observed for all bearings evaluated.
- Varying the externally applied radial load did not significantly impact bearing heat generation.
- Increasing oil flow to the test bearings resulted in increased heat generation.
- Roller slippage did not result in unusual thermal behavior of the test bearings nor did it produce visually obvious skid damage or distress at least for the duration of testing or the conditions imposed in this program.
- Experimental thermal performance data showed good correlation with the predictions made with the 3.0 MDN Roller Bearing Design System developed under NAPC Contract No. N00140-76-C-0383.

RECOMMENDATIONS

Based upon the above conclusions, the contractor makes the following recommendations:

- For minimum wear of high speed cylindrical roller bearings of the size range evaluated under this program, roller end clearance should be specified at or near the intermediate level evaluated.
- Both roller end circular runout and inner ring guide flange height should be maintained at the maximum levels evaluated in order to minimize roller and guide flange wear.
- The roller flat centrality tolerance can be maintained at the baseline level evaluated without concern for roller or guide flange wear.
- Bearing temperature monitoring should not be relied upon as a method to detect roller wear.
- Further tests are required in order to assess the long term effects of roller slippage on both skid damage and wear of the roller ends and guide flanges.

SECTION V LIST OF SYMBOLS

b	—Coefficient estimated from experimental data
b_1	—Calculated value of regression coefficient
DN	—Bearing bore diameter in millimeters multiplied by the bearing inner ring speed in revolutions per minute.
e	—Difference between observed and estimated value of the dependent variable due to residual variation or experimental error in observation.
N	—Sample size
QOIL	—Predicted Value of Bearing Oil Heat Generation.
QOILT	—Experiment Value of Bearing Oil Heat Generation.
$S_{y.i}$	—Standard error coefficient
T	—Student Table T-Value
TIR	—Predicted value of inner ring temperature.
TIRT	—Experimental value of inner ring temperature.
TOR	—Predicted value of outer ring temperature.
TORT	—Experimental value of outer ring temperature.
VAR 1	—Roller End Circular Runout
VAR 2	—Roller Flat Centralty
VAR 3	—Roller End Clearance
VAR 4	—Inner Ring Guide Flange Height
VAR 5	—Curvilinear effect of roller end clearance on roller weight loss.
VAR 6	—Curvilinear effect of roller end clearance on roller skew angle change.
X	—Value of the independent variable
\hat{Y}	—Value of the dependent variable
Y_1	—Average Weight Change
Y_2	—Average Skew Angle Change

REFERENCES

1. P&WA Interim Report FR-8615, "Development of Mainshaft High Speed Cylindrical Roller Bearings for Gas Turbine Engines," April 1977.
2. P&WA Interim Report FR-11453, "Development of Mainshaft High Speed Cylindrical Roller Bearings for Gas Turbine Engines," October 1978.